η and η' meson production in charmonium radiative decays

Extending $J/\psi \to \gamma\eta^{(\prime)}$ to decays of the axial—vector charmonium h_c

Mischa Batelaan

[hep-lat 2607.25707]
[MB Dudek Edwards PRL 135 161904]
[MB Dudek Edwards PRD 112 074505]

43rd International Symposium on Lattice Field Theory
29 July 2026, UMD

Charmonium radiative decays

- The electron positron collider at BESIII has produced a large amount of charmonia
  - ~10 billion J/ψ decays
  - ~3 billion $\psi(3686)$ decays
  - h_c accessed through $\pi^0 h_c$ decay of the $\psi(3686)$
  - Clean, gluon-rich production

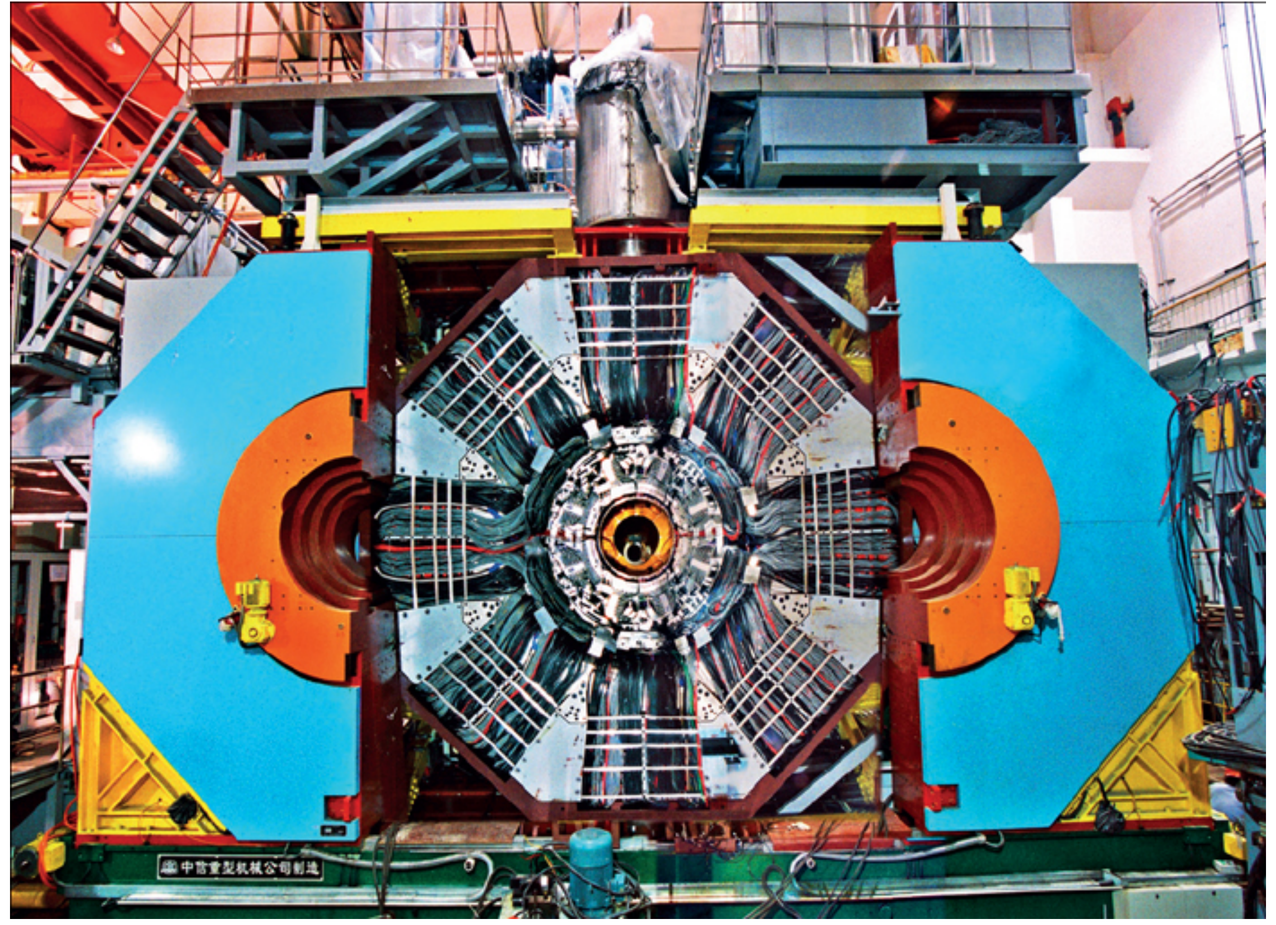

BESIII spectrometer in Beijing

Recently BESIII found an exotic hybrid isoscalar resonance in the radiative decay $J/\psi \to \gamma\eta\eta'$

Observation of an Isoscalar Resonance with Exotic $J^{PC} = 1^{-+}$ Quantum Numbers in $J/\psi \to \gamma\eta\eta'$

BESIII (2022) PRL 129 192002

$J/\psi \to \gamma\eta\eta'$

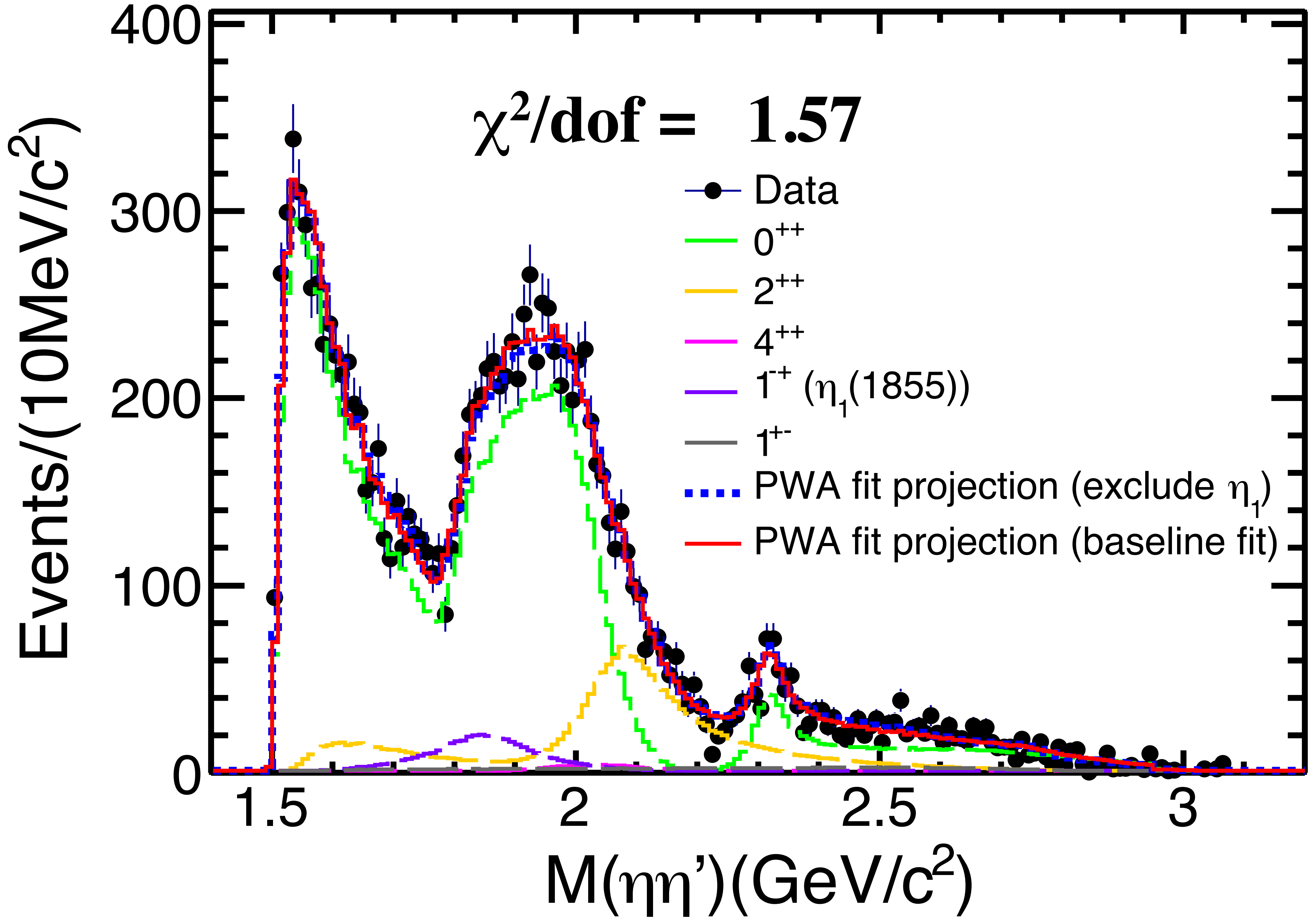

Charmonium radiative decays in lattice QCD

How do we calculate such decays in lattice QCD?

three-point functions: $\langle 0|\mathcal{O}_\eta(\Delta t)\mathcal{O}_\gamma(t)[\mathcal{O}_{J/\psi}(0)]^\dagger|0\rangle$

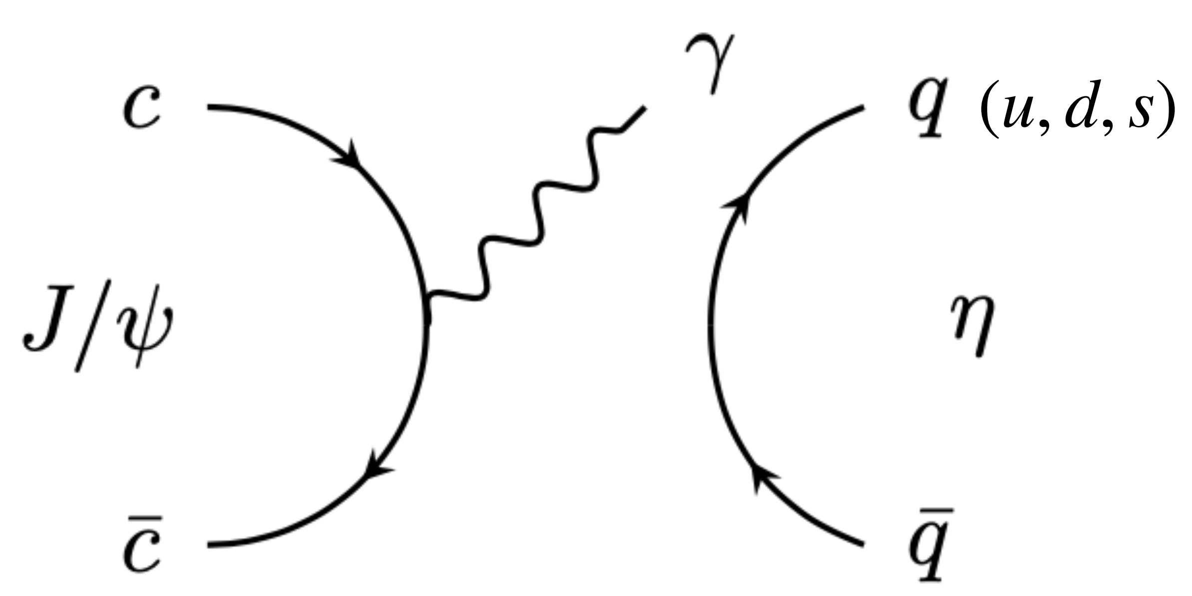

Challenges:

- Disconnected diagrams (noisy!)
- Need to access both the η and η'
  - Requires distinct light and strange quarks $(N_f = 2 + 1)$
- η' and h_c appear as excited states in some irreps
  - We need optimized operators to access these states
- Mass gap is large between the mesons: $m_{J/\psi} - m_\eta \approx 2.4$ GeV.
  - We need operators at large momenta for all mesons to access $Q^2 = 0$

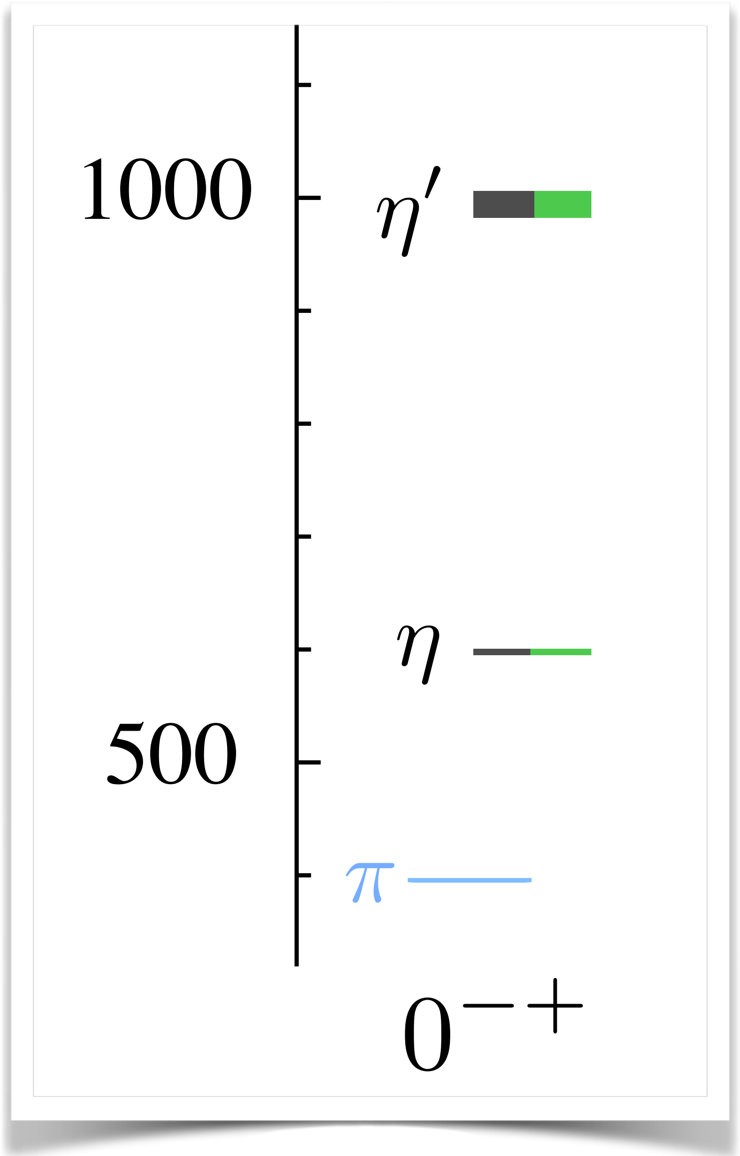

Lattice QCD tools

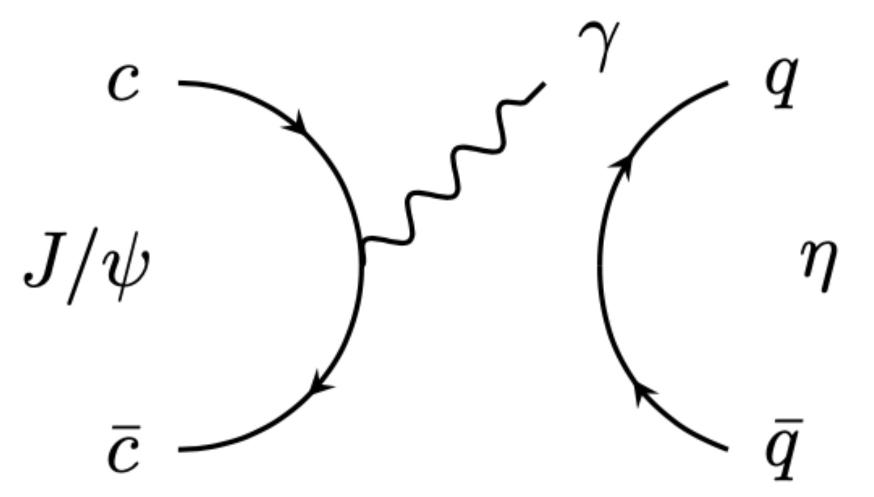

$L^3 \times T^3$	20×256
N_{cfgs}	288
N_{vec}	128
m_π	391 MeV
ξ	3.5
a_s	0.12fm

$$\xi = \frac{a_s}{a_t}$$

<u>We need:</u>

- Definite momentum operators
- quark annihilation lines
- optimized operators using a large basis

→ Distillation

- Construct operators by coupling Γ in spherical basis with derivatives:

$$\mathcal{O} = \bar{\psi}\Gamma D \ldots D\psi$$

- Operators will be in irreducible representations of the cubic group

- In-flight operators will mix parities:

Meson	J^{PC}	$[n00]$			$[nn0]$				$[nnn]$		
		A_1	A_2	E_2	A_1	A_2	B_1	B_2	A_1	A_2	E_2
$J/\psi, \psi'$	1^{--}	0		1	0		1	1	0		1
h_c	1^{+-}		0	1		0	1	1		0	1

Energy spectrum & optimized operators

- Construct matrix of two-point correlators using a large operator basis $\{\mathcal{O}_i\}$
- Diagonalize the matrix with GEVP and extract energy levels E_n by fitting the eigenvalues
- Construct optimized operators for each state as a linear combination of the operator basis

$$\Omega_n^\dagger = \sqrt{2E_n} e^{-E_n t_0/2} \sum_i (v_n)_i \mathcal{O}_i^\dagger$$

- Independently determine optimized operator for each momentum value

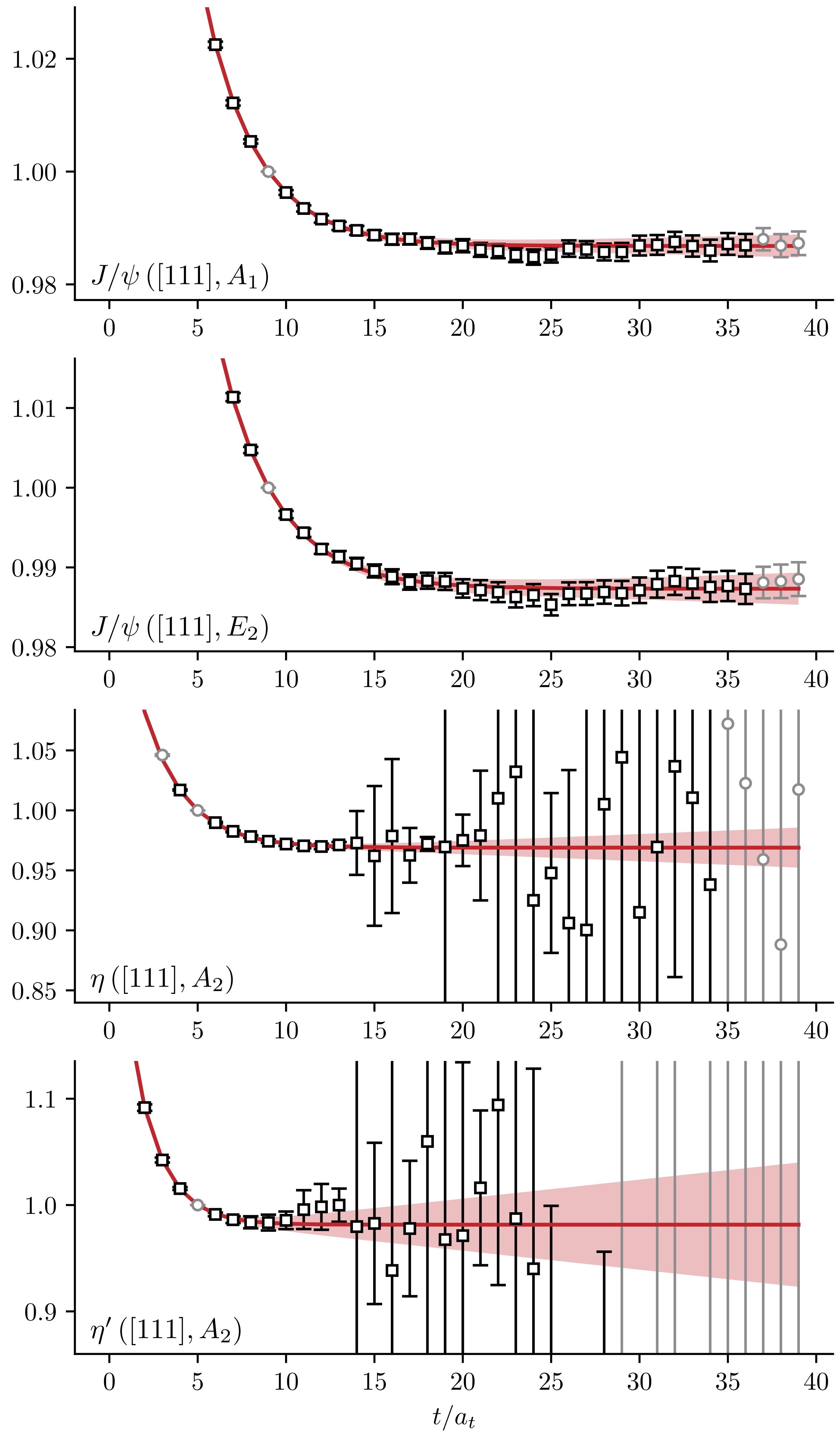

Optimized operators

Fit to the energies with dispersion relation determines the anisotropy $\xi \approx 3.5$

charmonia $(J/\psi, h_c, \psi')$

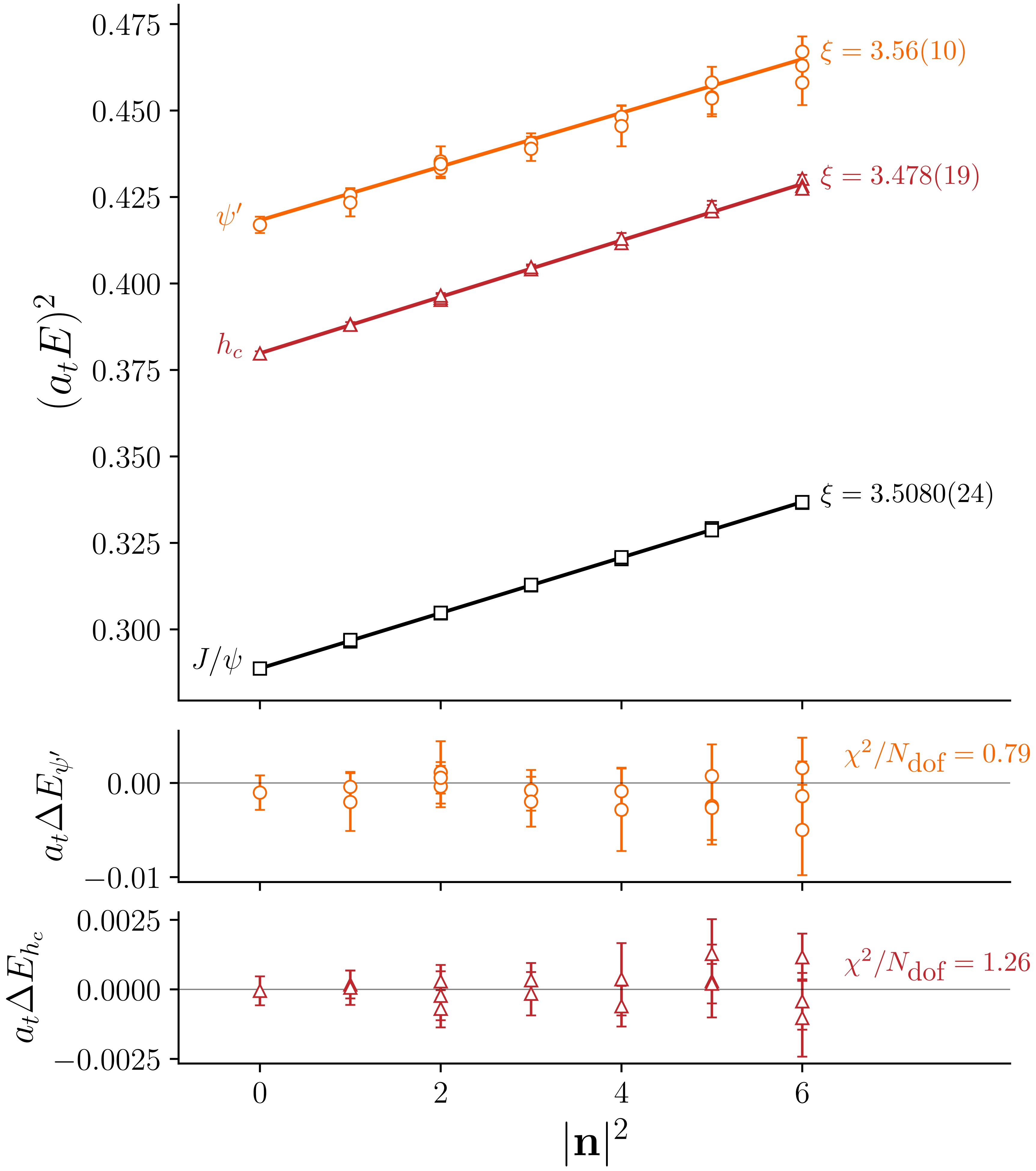

Using bases of 21–35 operators for momenta up to $|\vec{n}|^2 \leq 6$.

light pseudoscalars (η, η')

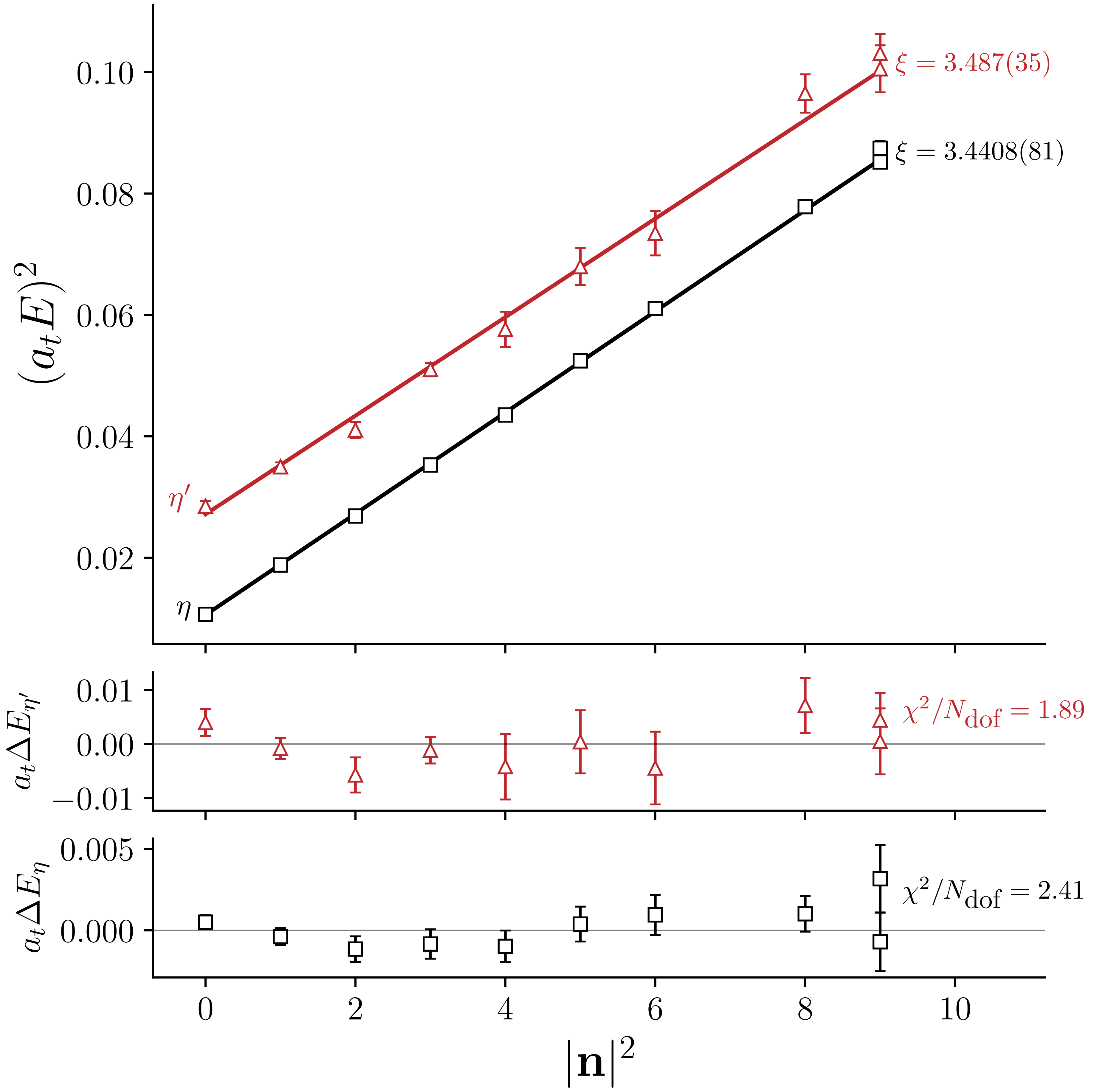

Using bases of 32–61 operators for momenta up to $|\vec{n}|^2 \leq 9$.

Three-point functions

We can use the optimized operators in a three-point function:

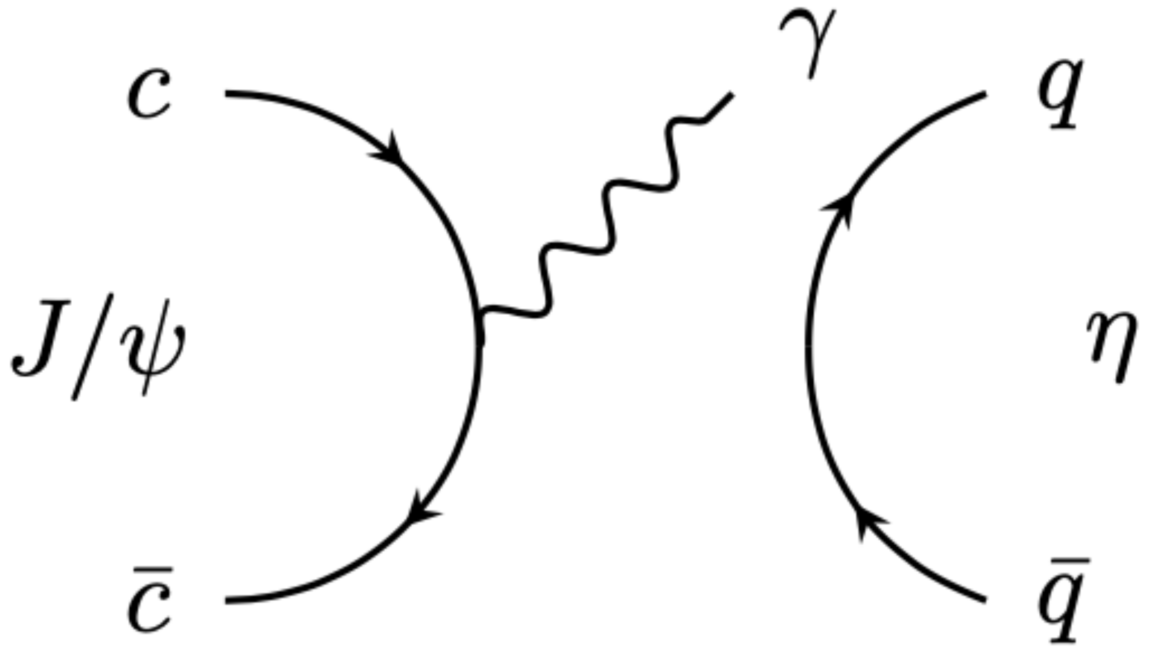

$$\langle 0 | \, \Omega_{\eta^{(\prime)}}^{\mathbf{p}'\Lambda'\mu'}(\Delta t) \; \underbrace{j^{\mathbf{q}\Lambda_\gamma\mu_\gamma}(t)} \; \left[\Omega_{\psi}^{\mathbf{p}\Lambda\mu}\right]^\dagger(0) \, |0\rangle$$

Sink operator with all possible momentum rotations $|\vec{n}|^2 \leq 6$

- Restrict momenta to canonical types up to $|\vec{n}|^2 \leq 16$
- Use the $\mathcal{O}(a)$-improved vector current
- Renormalization constant from previous work
  JHEP 05 (2024) 230

Source operator with all possible momentum directions $|\vec{n}|^2 \leq 4$

$\frac{a_s L}{2\pi}\vec{q}$
$(0,0,0)$
$(0,0,n)$
$(0,n,n)$
(n,n,n)
$(0,m,n)$
(m,n,n)

Use matrix element decomposition to find all non-zero operator combinations

$$C_3 \propto K(\{\Lambda\},\{\mu\},\{\vec{p}\}) \cdot F(Q^2)$$

Wigner-Eckart theorem

Wigner-Eckart theorem relates each matrix elements to a *reduced matrix element*:

$$\underbrace{\langle 0 | \, \Omega_{\eta^{(\prime)}}^{\{\mathbf{p}'\}^\star_{k'}\Lambda'\mu'} \cdot j^{\mathbf{q}\Lambda_\gamma\mu_\gamma} \cdot \left[\Omega_{\psi}^{\{\mathbf{p}\}^\star_k\Lambda\mu}\right]^\dagger | 0 \rangle}_{} = \underbrace{\mathcal{C}\big(\{\mathbf{p}\}^\star_k\Lambda\mu;\, \{\mathbf{p}'\}^\star_{k'}\Lambda'\mu';\, \mathbf{q}\,\Lambda_\gamma\mu_\gamma\big)}_{} \cdot \underbrace{\mathbb{C}\big(\{\mathbf{p}'\}^\star\Lambda'; \mathbf{q}\Lambda_\gamma; \{\mathbf{p}\}^\star\Lambda\big)}_{}$$

Combinations of all

- allowed lattice rotations of the momenta
- rows of the irreps

Clebsch-Gordan coeff.

reduced correlator

Wigner-Eckart theorem

Wigner-Eckart theorem relates each matrix elements to a *reduced matrix element*:

$$\underbrace{\left\langle 0 \right| \Omega_{\eta^{(\prime)}}^{\{\mathbf{p}'\}^\star_{k'}\Lambda'\mu'} \cdot j^{\mathbf{q}\Lambda_\gamma\mu_\gamma} \cdot \left[\Omega_{\psi}^{\{\mathbf{p}\}^\star_{k}\Lambda\mu}\right]^\dagger \left| 0 \right\rangle}_{\text{Combinations of all}} = \underbrace{\mathcal{C}\left(\{\mathbf{p}\}^\star_k\Lambda\mu;\ \{\mathbf{p}'\}^\star_{k'}\Lambda'\mu';\ \mathbf{q}\,\Lambda_\gamma\mu_\gamma\right)}_{\text{Clebsch-Gordan coeff.}} \cdot \underbrace{\mathbb{C}\left(\{\mathbf{p}'\}^\star\Lambda';\mathbf{q}\Lambda_\gamma;\{\mathbf{p}\}^\star\Lambda\right)}_{\text{reduced correlator}}$$

Combinations of all
- allowed lattice rotations of the momenta
- rows of the irreps

Example using $J/\psi \to \gamma\eta_c$:

μ_{η_c}	μ_γ	$\mu_{J/\psi}$	$\left\langle P_{A_2},\mu_{\eta_c}; j_{T_1^-},\mu_\gamma \middle| V_{E_2};\mu_{J/\psi}\right\rangle$
1	1	2	$\frac{1}{2\sqrt{3}}$
1	3	2	$\frac{i}{2\sqrt{3}}$
1	1	1	$\frac{1}{6}$
1	2	1	$\frac{1+i}{3\sqrt{2}}$
1	3	1	$-\frac{i}{6}$

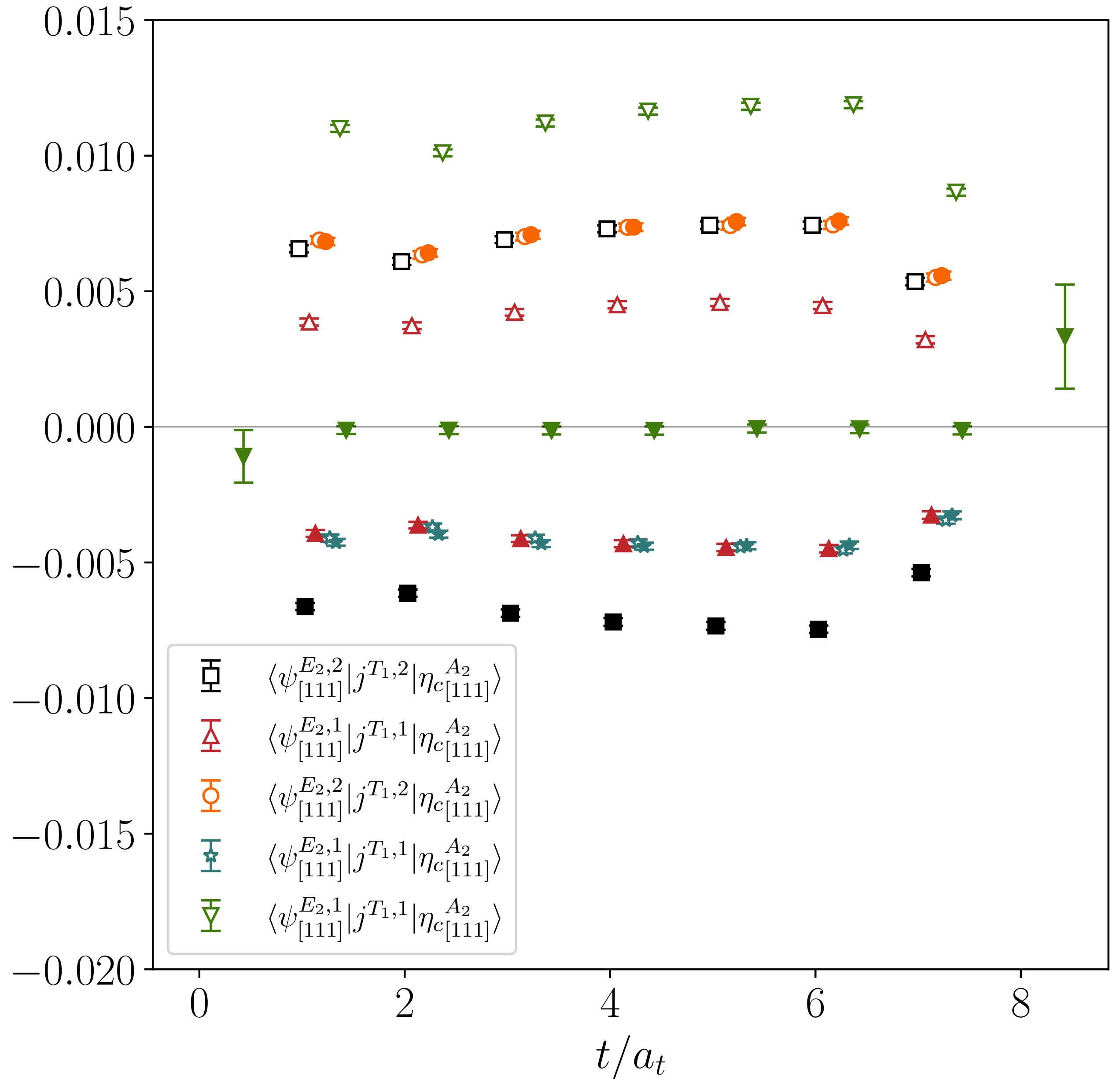

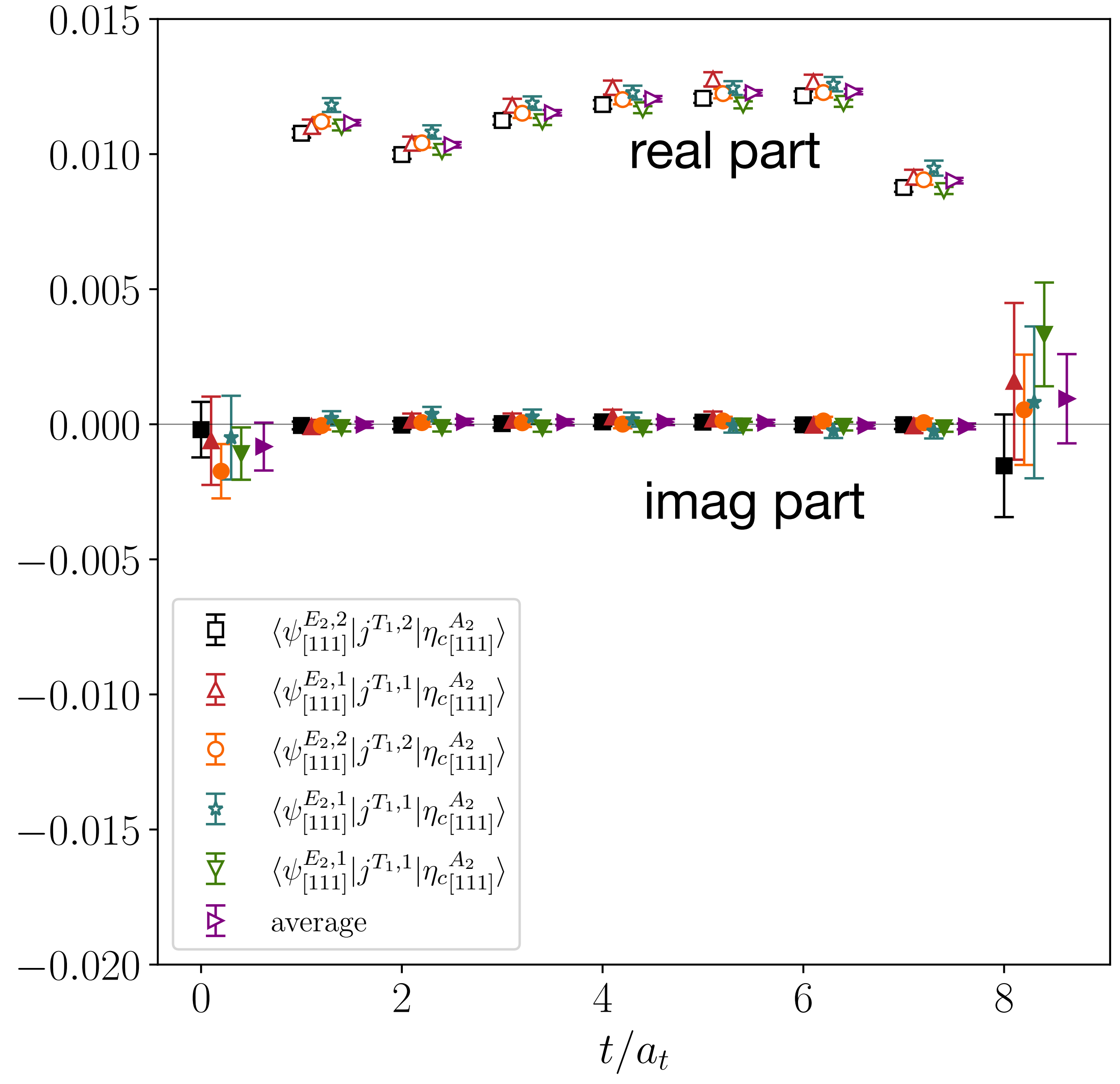

Fitting method

- Divide out the time-dependence:

$$\tilde{C}(t,\Delta t) \equiv \frac{\sqrt{2E_{\eta^{(\prime)}}\,2E_{\psi}}}{e^{-E_{\eta^{(\prime)}}(\Delta t - t)}e^{-E_{\psi}t}}\,C(t,\Delta t)$$

- Fit with variations of

$$R(t_\gamma) = C + A_{\rm src}e^{\delta E_{\rm src}t_\gamma} + A_{\rm snk}e^{\delta E_{\rm snk}(t_f - t_\gamma)}$$

over different time-windows.

- Take model average with AIC weighting, using the 30 best fits.

- Four different source-sink separations $\Delta t/a_t = \{12, 16, 20, 24\}$ to check consistency.

$\vec{n}_{\eta'} = (0,0,-2), \vec{n}_{J/\psi} = (0,0,2)$

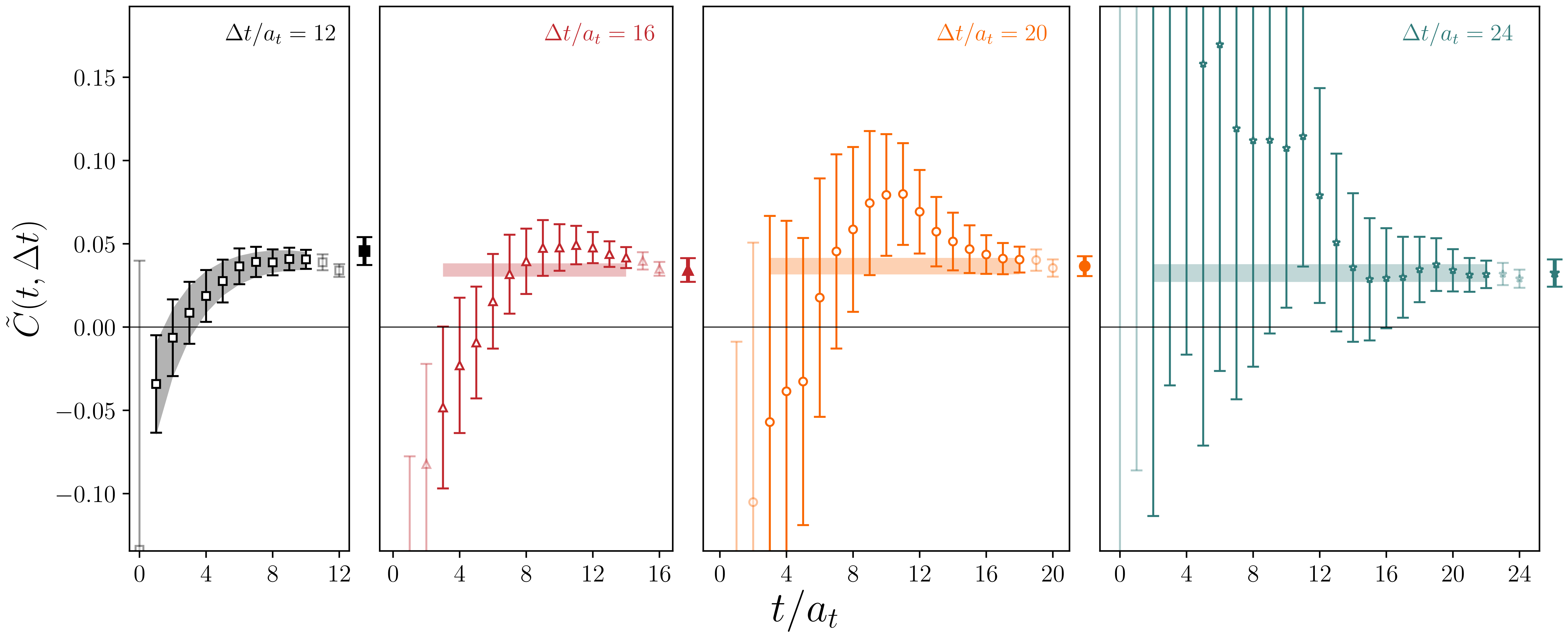

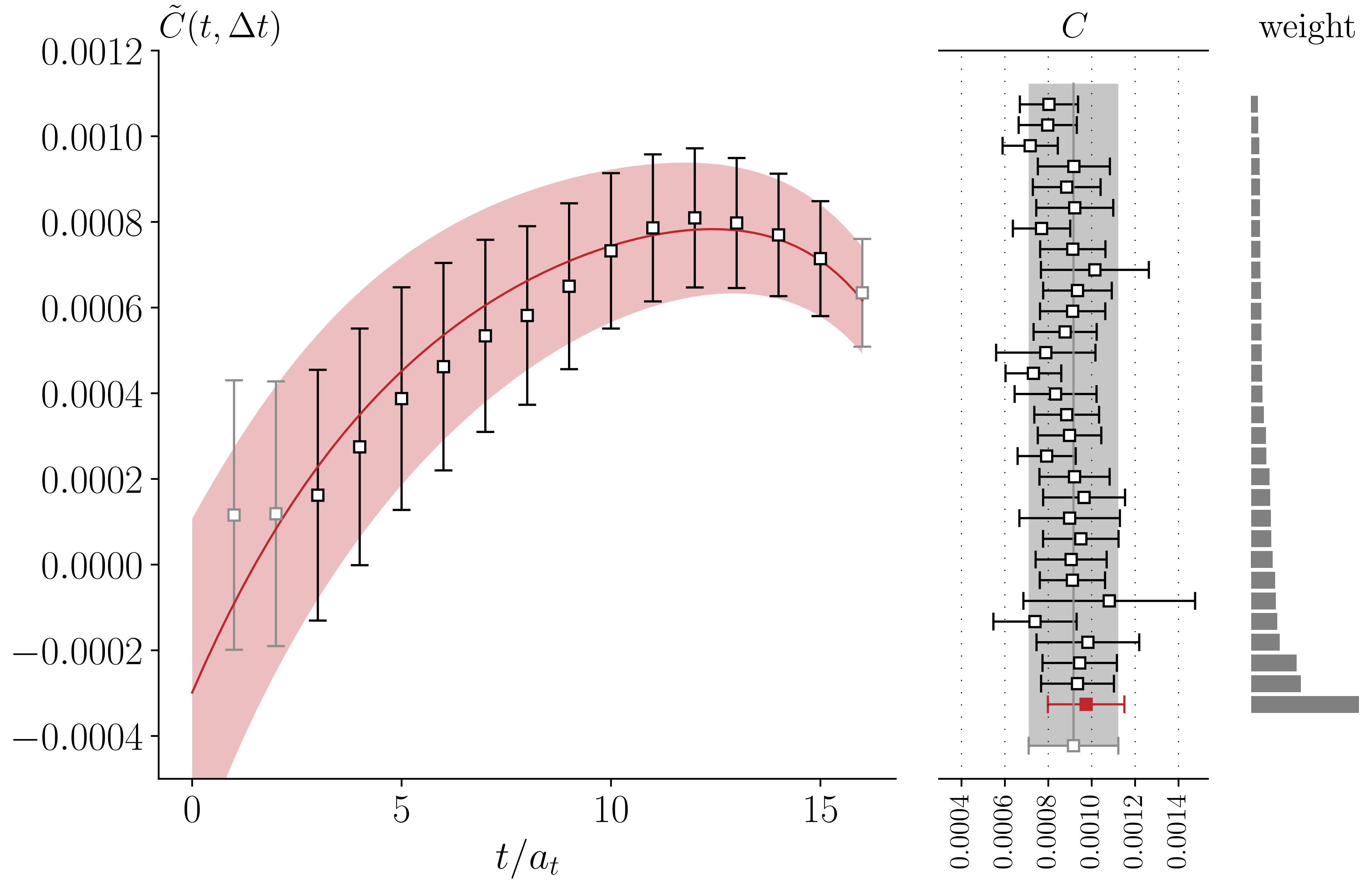

$J/\psi \to \gamma\eta^{(\prime)}$ Transition Form Factors

$$\langle \eta^{(\prime)}(\mathbf{p}') | j^{\mu}_{\mathrm{em}}(0) | J/\psi(\mathbf{p},\lambda) \rangle = \epsilon^{\mu\nu\rho\sigma}\, p'_{\nu}\, p_{\rho}\, \epsilon_{\sigma}(\mathbf{p},\lambda)\, F_{\psi\eta^{(\prime)}}(Q^2)$$

$\boxed{\text{1748 correlators}} \xrightarrow{\text{W-E avg. \& fitting}} \boxed{\text{276 matrix elements}} \xrightarrow{\text{Solve for FF at each } Q^2} \boxed{\text{70 } Q^2 \text{ points}}$

$J/\psi \to \gamma\eta^{(\prime)}$ Transition Form Factors

$$\langle \eta^{(\prime)}(\mathbf{p}')|j^{\mu}_{\mathrm{em}}(0)|J/\psi(\mathbf{p},\lambda)\rangle = \epsilon^{\mu\nu\rho\sigma}\, p'_{\nu}\, p_{\rho}\, \epsilon_{\sigma}(\mathbf{p},\lambda)\, F_{\psi\eta^{(\prime)}}(Q^2)$$

$\boxed{\text{1748 correlators}} \xrightarrow{\text{W-E avg. \& fitting}} \boxed{\text{276 matrix elements}} \xrightarrow{\text{Solve for FF at each } Q^2} \boxed{70\ Q^2 \text{ points}}$

$J/\psi \to \gamma\eta$

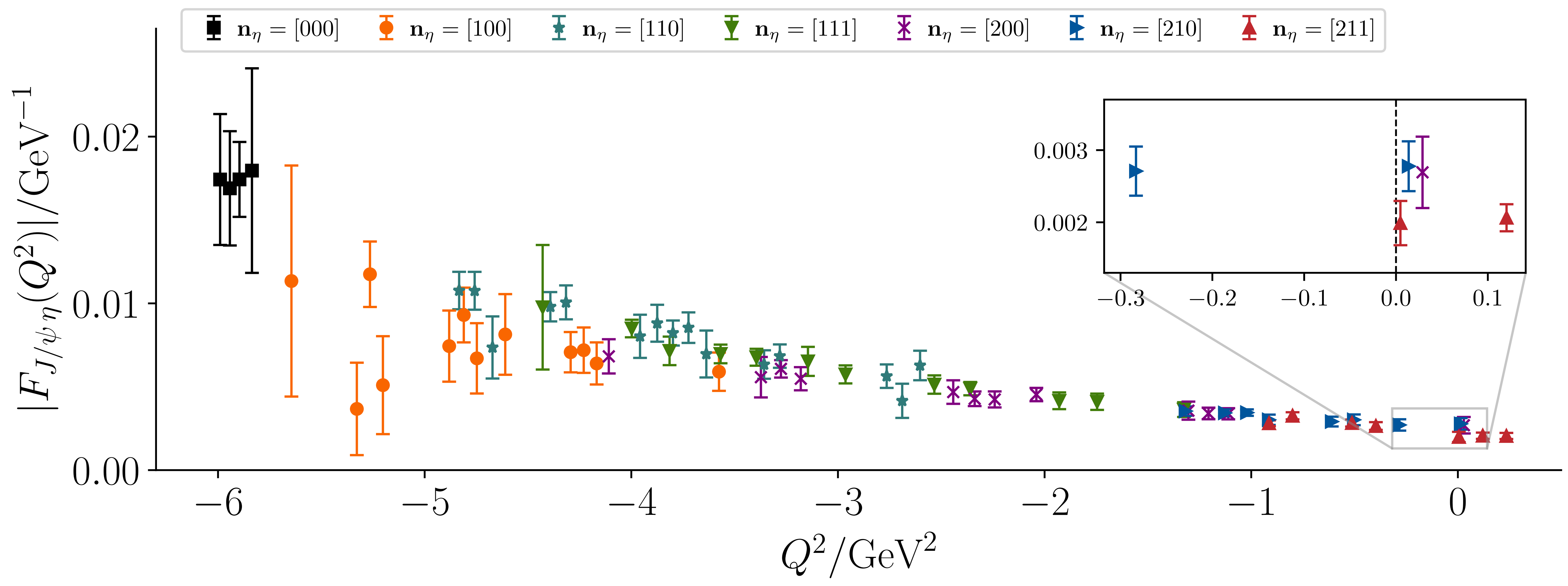

$J/\psi \to \gamma\eta'$

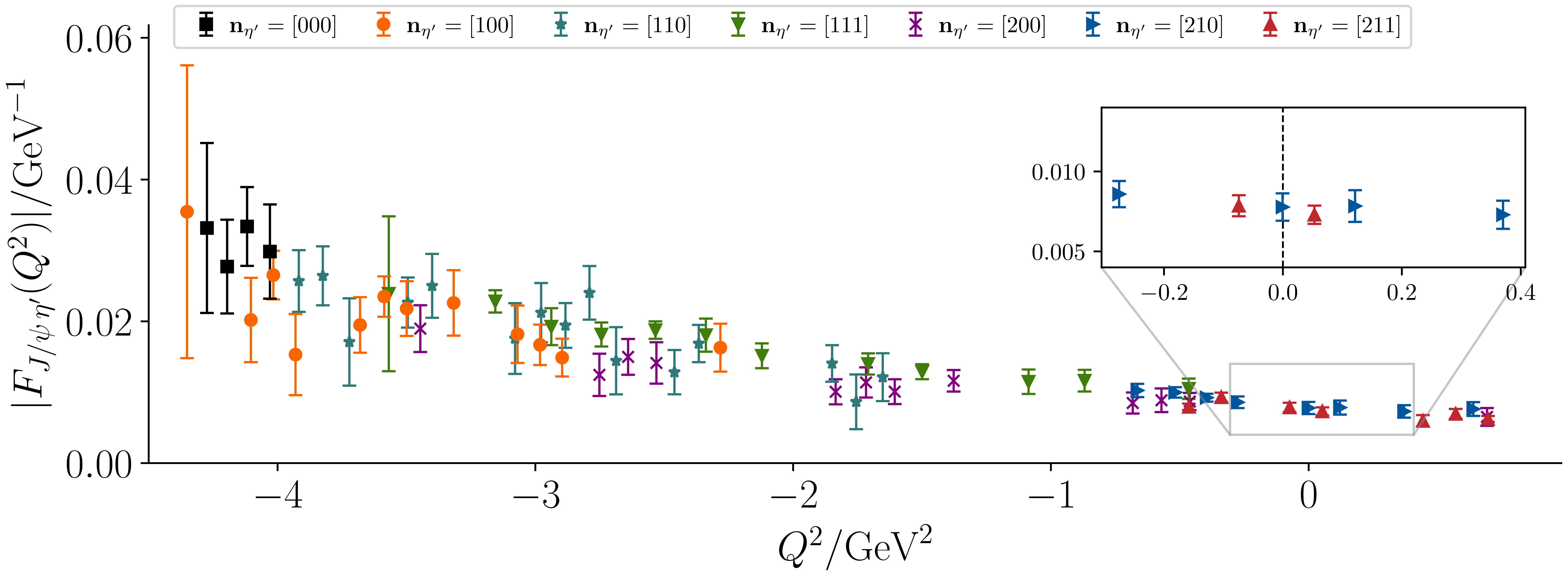

High-momentum operators are essential to reach $Q^2 = 0$

Comparison with BESIII experimental results

- Partial decay rates can be expressed as

$$\Gamma(J/\psi \to \gamma\eta^{(\prime)}) = \frac{4\alpha}{27}|\vec{q}|^3|\hat{F}_{J/\psi\,\eta^{(\prime)}}(0)|^2$$

$$|\vec{q}| = \frac{m_{J/\psi}^2 - m_\eta^2}{2m_{J/\psi}} \qquad F(Q^2) = \frac{2}{3}\,e\,\hat{F}(Q^2)$$

- Best estimate: linear fit around $Q^2 = 0$ with sys. error due to variation in anisotropy ξ.

- Gluonic intermediate state can only reach the $SU(3)_{flav.}$ singlet
  - We expect the decay to η' to have a larger amplitude than to η

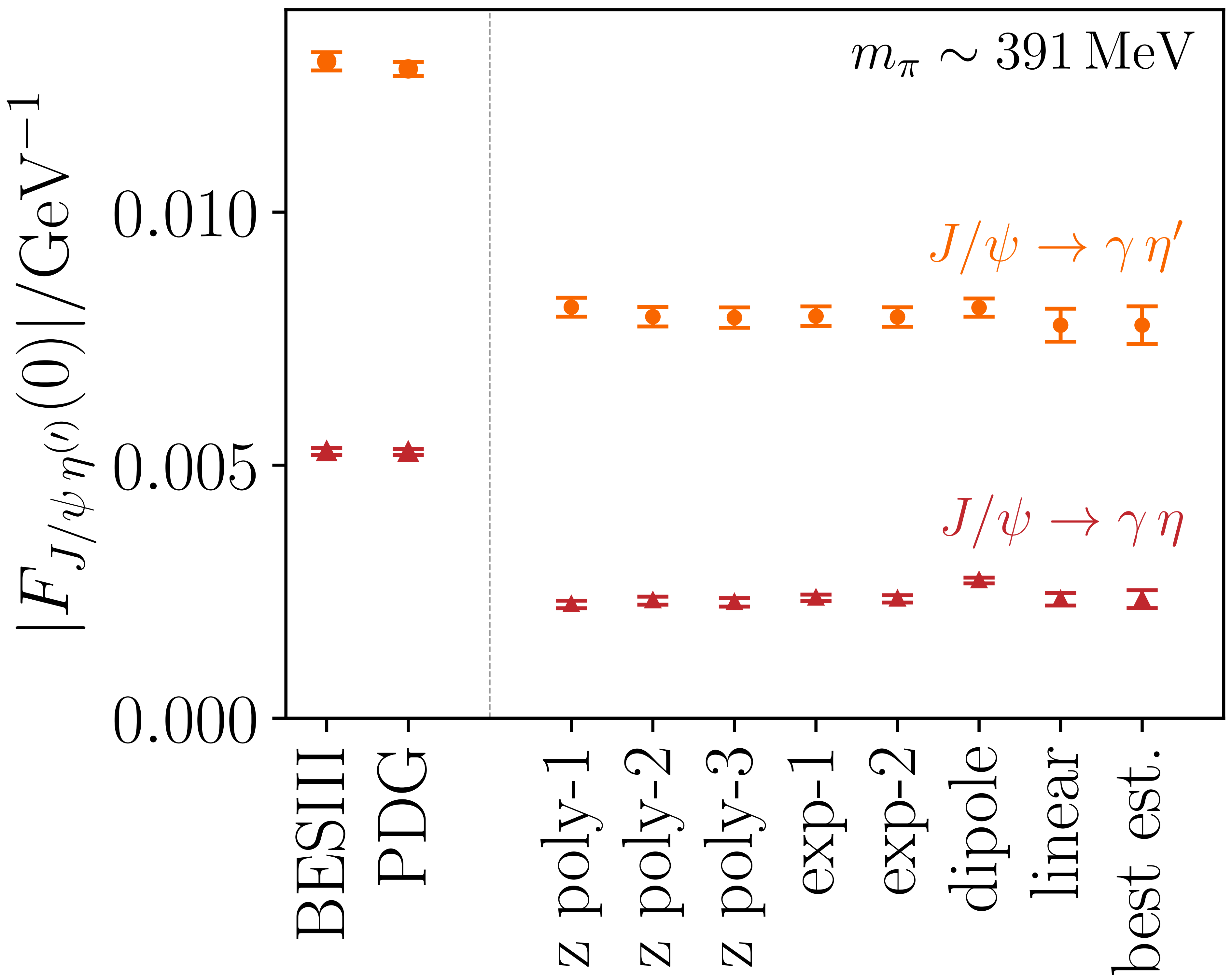

Discrepancy with experiment

vacuum topology? light quark mass? $U(1)_A$ anomaly?

BESIII (2023) PRD 108 092002

$h_c \to \gamma\eta^{(\prime)}$ radiative decays $\quad 1^{+-} \to 0^{-+}$

$$\langle \eta^{(\prime)}(\mathbf{p}') | j^\mu(0) | h_c(\mathbf{p},\lambda)\rangle = \Omega^{-1}(Q^2)\Big(E_1(Q^2)\big[\Omega(Q^2)\,\epsilon^\mu - (\epsilon\cdot p')\big((p\cdot p')\,p^\mu - m_{h_c}^2\,p'^\mu\big)\big]$$
$$+ C_1(Q^2)\,m_{h_c}(\epsilon\cdot p')\big[(p\cdot p')\,(p+p')^\mu - m_{\eta^{(\prime)}}^2\,p^\mu - m_{h_c}^2\,p'^\mu\big]\Big)$$

Two form factors: electric dipole $E_1(Q^2)$, and longitudinal $C_1(Q^2)$.

Heavier mass of the h_c pushes the η/η' to even larger momenta (out to $|n|^2 = 9$)

The h_c is an excited state in the helicity ± 1 irreps (it lies above the J/ψ).

- optimized operators are essential

Meson	J^{PC}	$[nn0]$ A_1	A_2	B_1	B_2
$J/\psi, \psi'$	1^{--}	0		1	1
h_c	1^{+-}		0	1	1

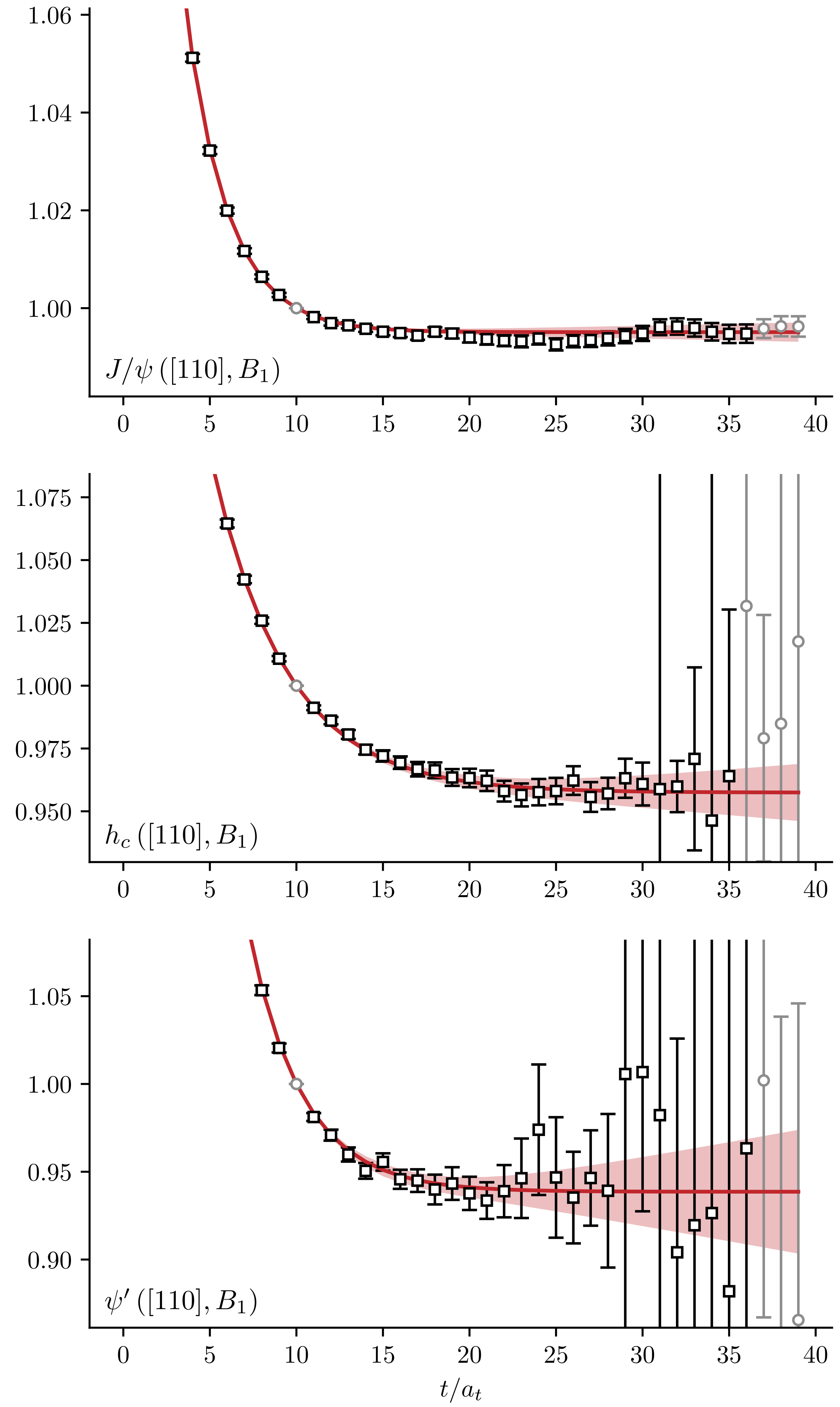

$h_c \to \gamma\eta^{(\prime)}$ radiative decays

$1^{+-} \to 0^{-+}$

electric dipole $E_1(Q^2)$, longitudinal $C_1(Q^2)$

$$\langle \eta^{(\prime)}(\mathbf{p}') | j^\mu(0) | h_c(\mathbf{p},\lambda)\rangle = \Omega^{-1}(Q^2)\Big(E_1(Q^2)\big[\Omega(Q^2)\,\epsilon^\mu - (\epsilon\cdot p')\big((p\cdot p')\,p^\mu - m_{h_c}^2\,p'^\mu\big)\big] + C_1(Q^2)\,m_{h_c}(\epsilon\cdot p')\big[(p\cdot p')\,(p+p')^\mu - m_{\eta^{(\prime)}}^2\,p^\mu - m_{h_c}^2\,p'^\mu\big]\Big)$$

Decay rate is set by $E_1(0)$ alone.

$$\Gamma(h_c \to \gamma\eta^{(\prime)}) = \frac{4}{27}\alpha\frac{|\mathbf{q}|}{m_{h_c}^2}\big|E_1(0)\big|^2$$

$$\Gamma_i = \sum_j K_{ij}(\mathbf{p}'\Lambda';\, \mathbf{q}\Lambda_\gamma\mu_\gamma;\, \mathbf{p}\Lambda\mu)\cdot F_j(Q^2)$$

At each Q^2 point, solve the overconstrained system for the form factors

$$\mathbf{F} = \left(\mathbf{K}^T\mathbf{\Sigma}^{-1}\mathbf{K}\right)^{-1}\mathbf{K}^T\mathbf{\Sigma}^{-1}\,\mathbf{\Gamma}$$

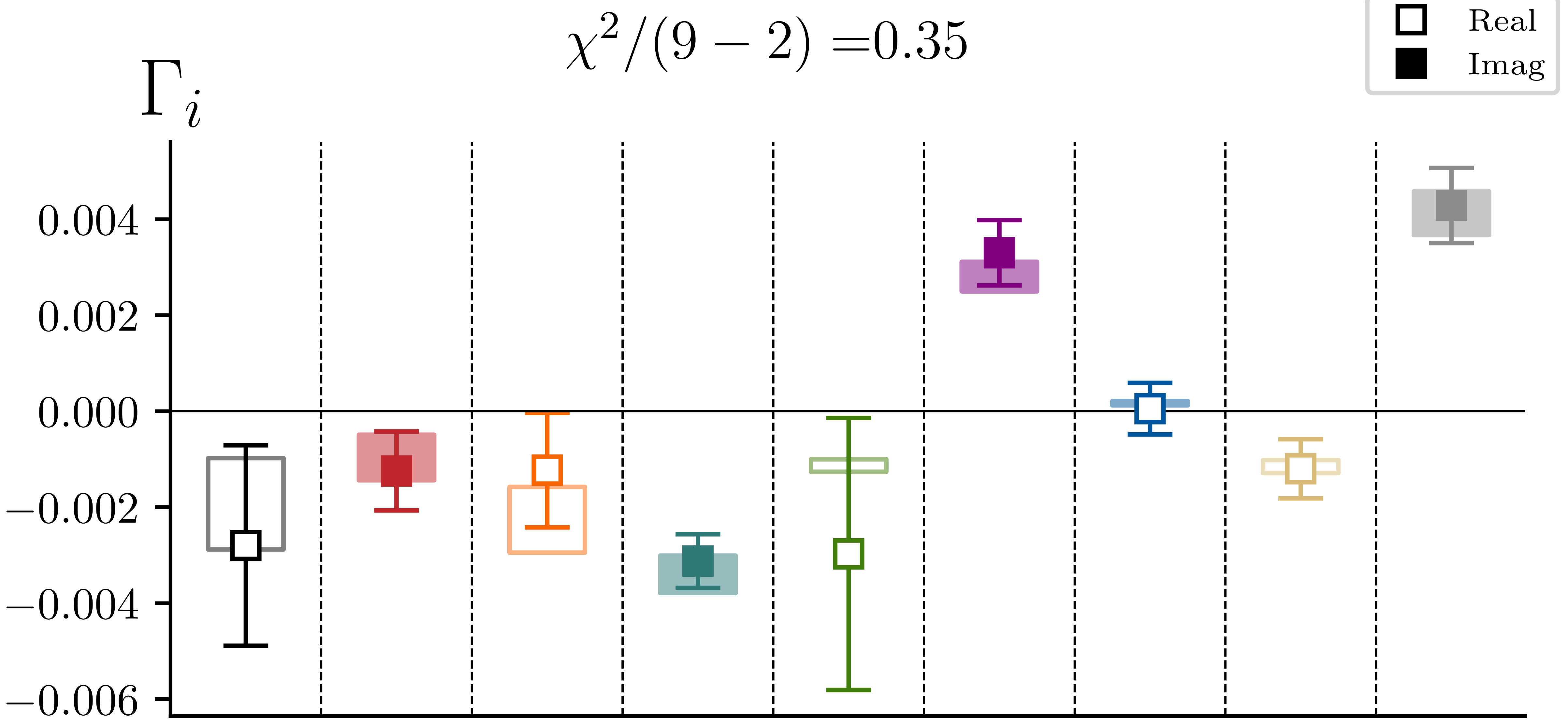

Simultaneous Fitting

$\vec{n}_{\eta'} = (-1,-1,-2), \vec{n}_{h_c} = (0,1,0)$

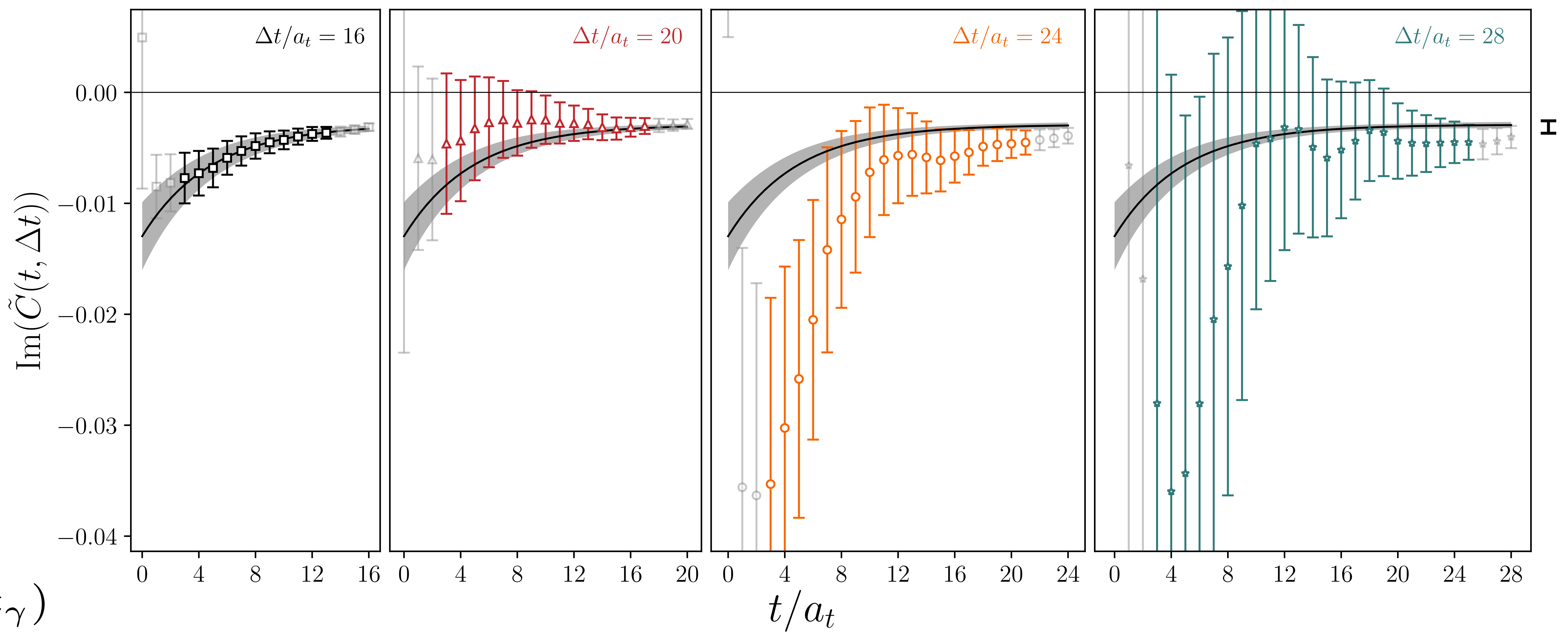

- Fit four source-sink separations $\Delta t/a_t = \{16, 20, 24, 28\}$ simultaneously
- Fit variations of

$$R(t_\gamma) = C + A_{\mathrm{src}} e^{\delta E_{\mathrm{src}} t_\gamma} + A_{\mathrm{snk}} e^{\delta E_{\mathrm{snk}}(t_f - t_\gamma)}$$

over different time-windows

Take model average with AIC weighting

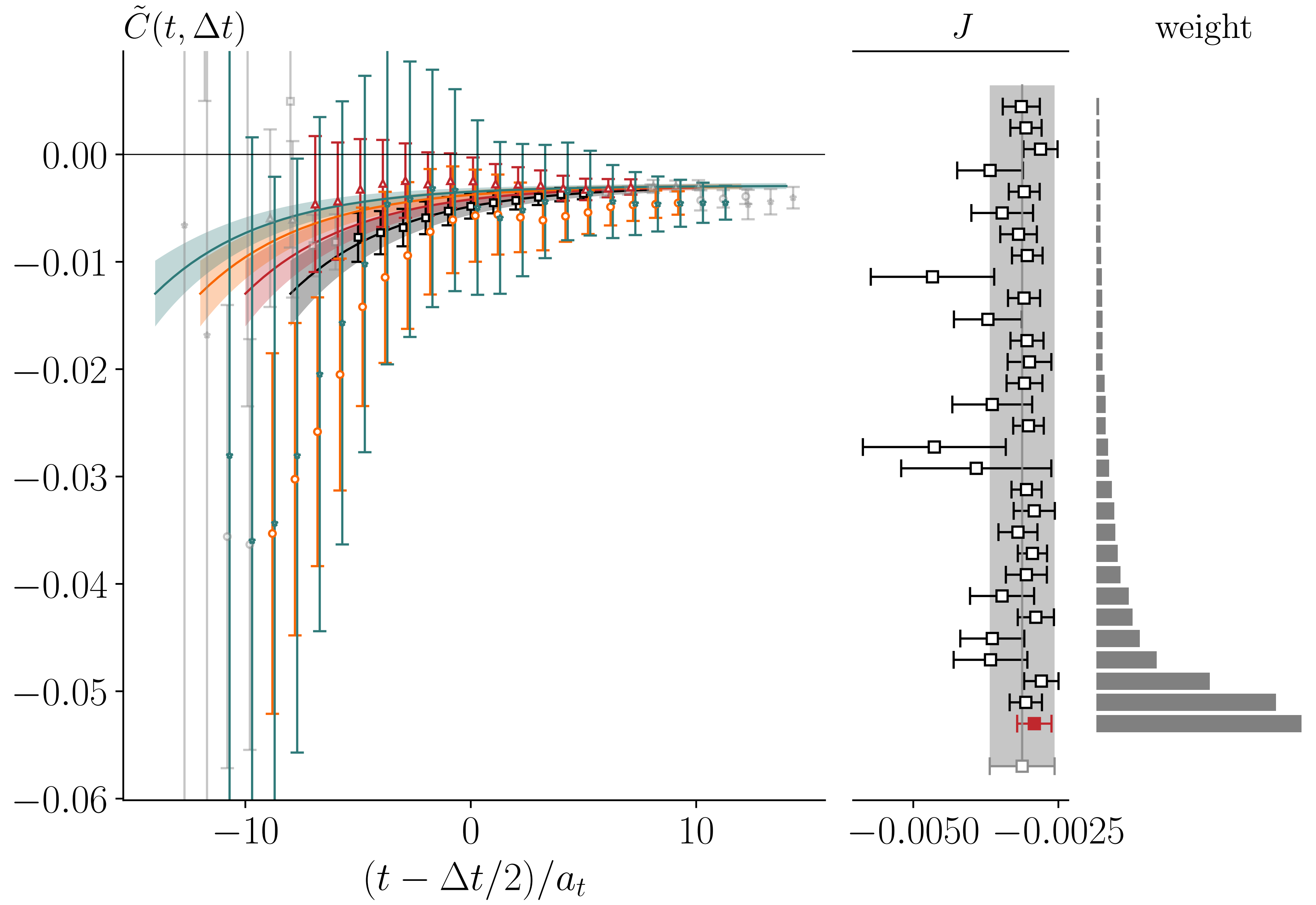

$h_c \to \gamma\eta^{(\prime)}$ radiative decays

$$\langle \eta^{(\prime)}(\mathbf{p}') | j^\mu(0) | h_c(\mathbf{p},\lambda)\rangle = \Omega^{-1}(Q^2)\Big(E_1(Q^2)\left[\Omega(Q^2)\,\epsilon^\mu - (\epsilon\cdot p')\big((p\cdot p')\,p^\mu - m_{h_c}^2\,p'^\mu\big)\right] + C_1(Q^2)\,m_{h_c}(\epsilon\cdot p')\left[(p\cdot p')\,(p+p')^\mu - m_{\eta^{(\prime)}}^2\,p^\mu - m_{h_c}^2\,p'^\mu\right]\Big)$$

$h_c \to \gamma\eta$

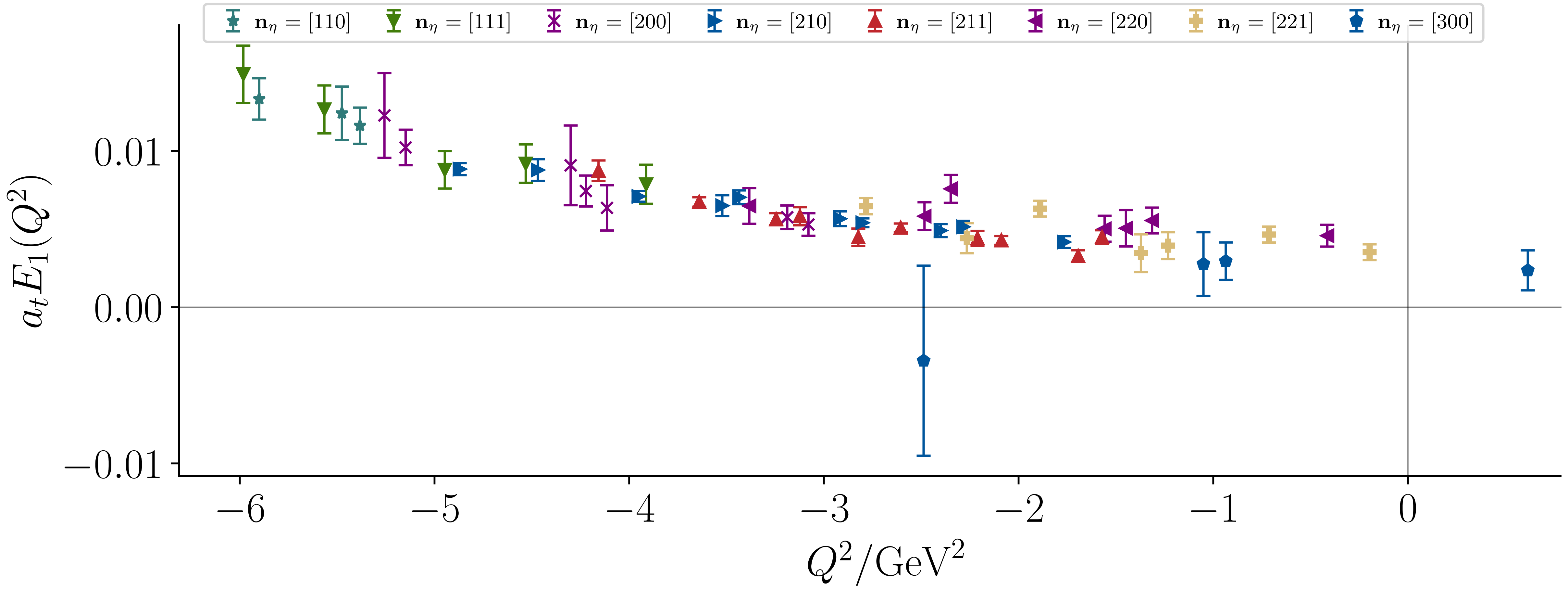

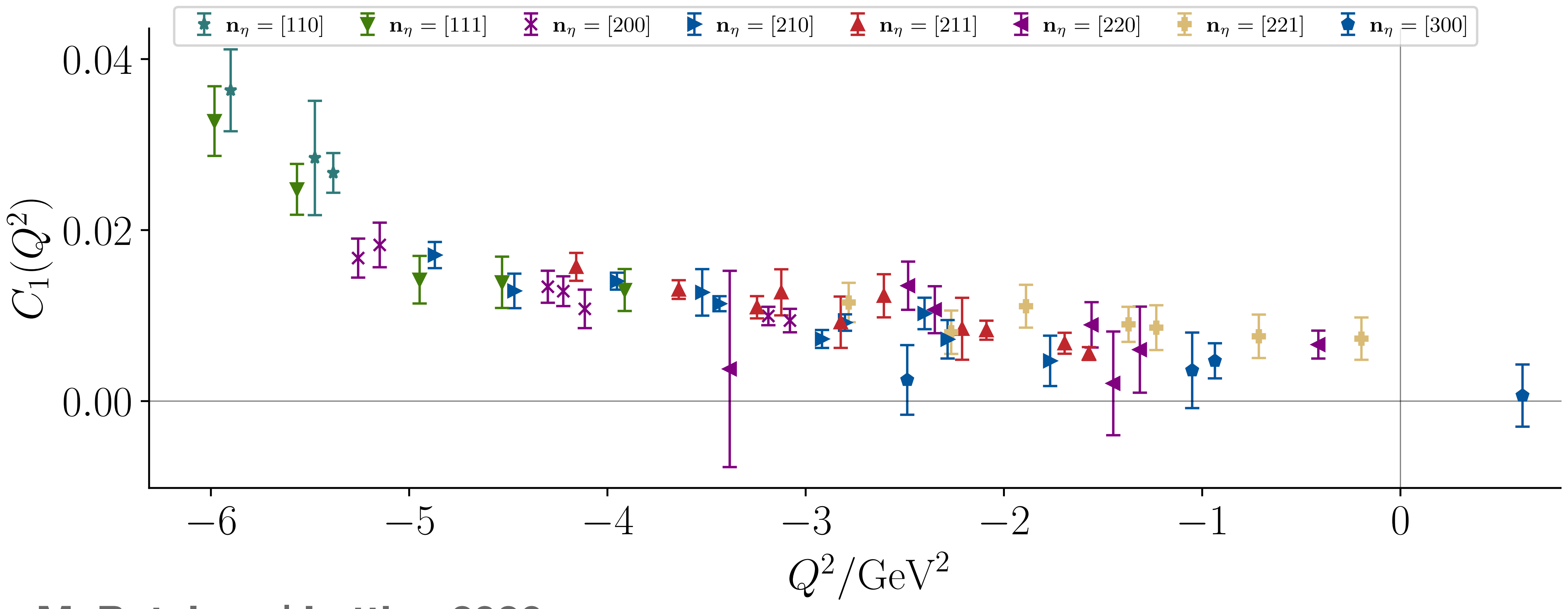

$h_c \to \gamma\eta'$

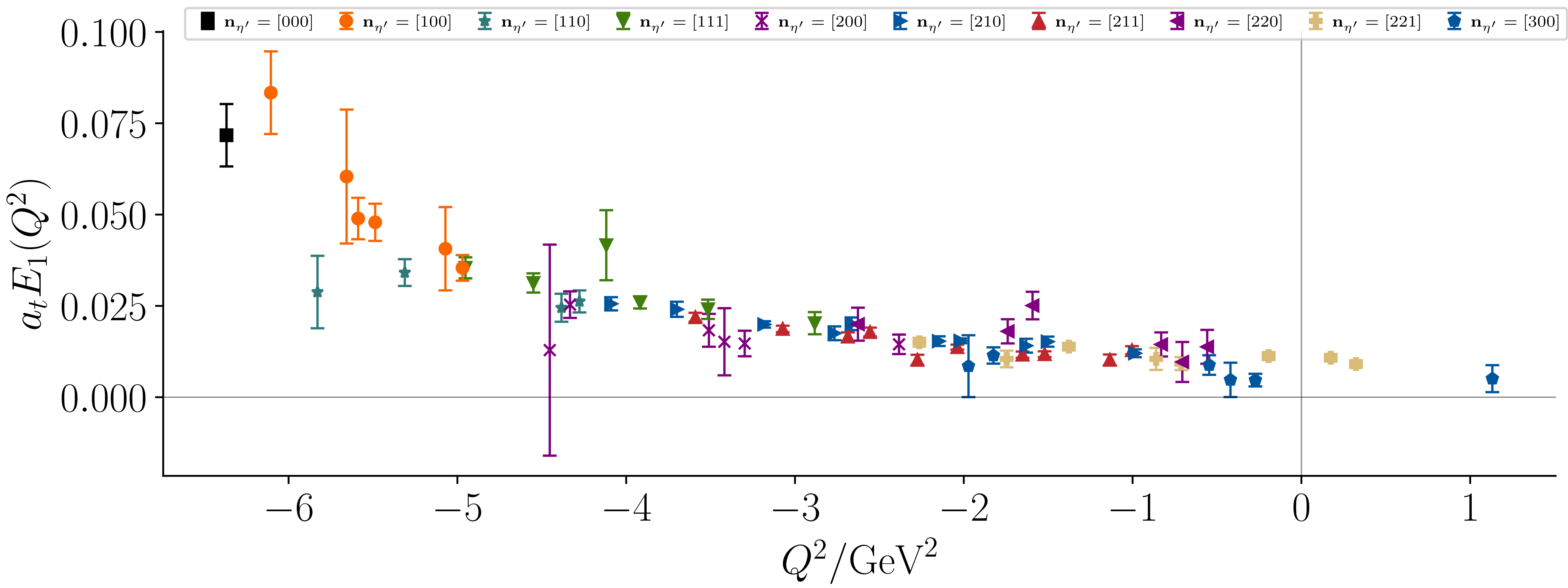

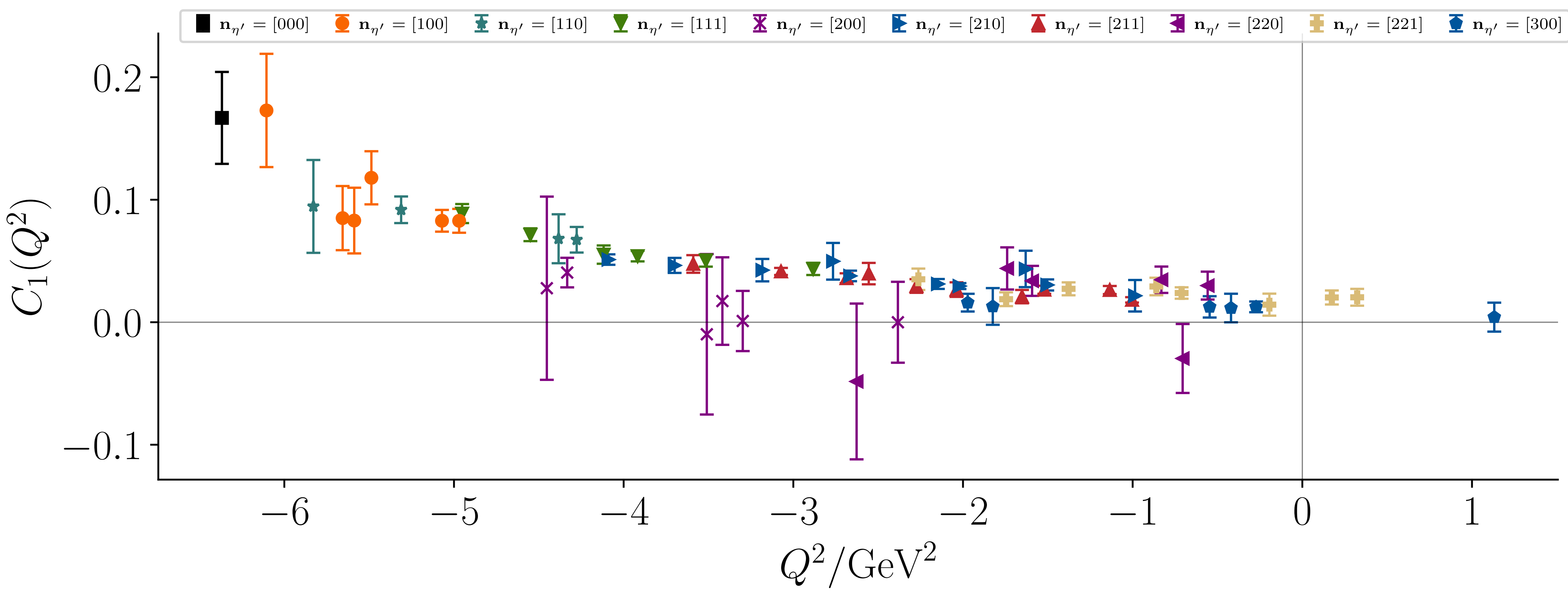

Comparison with BESIII results

Similar discrepancy with experiment for h_c radiative decays

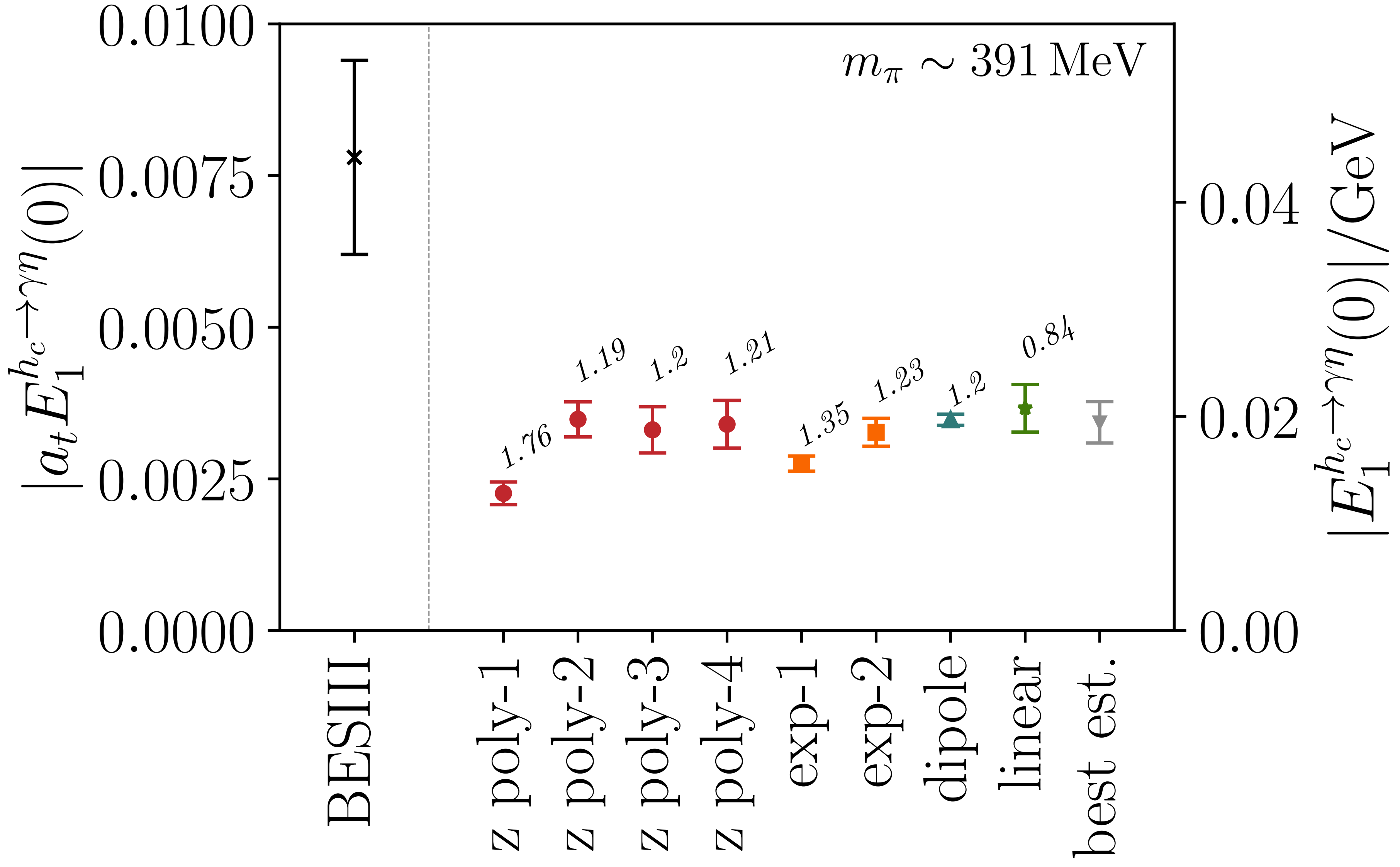

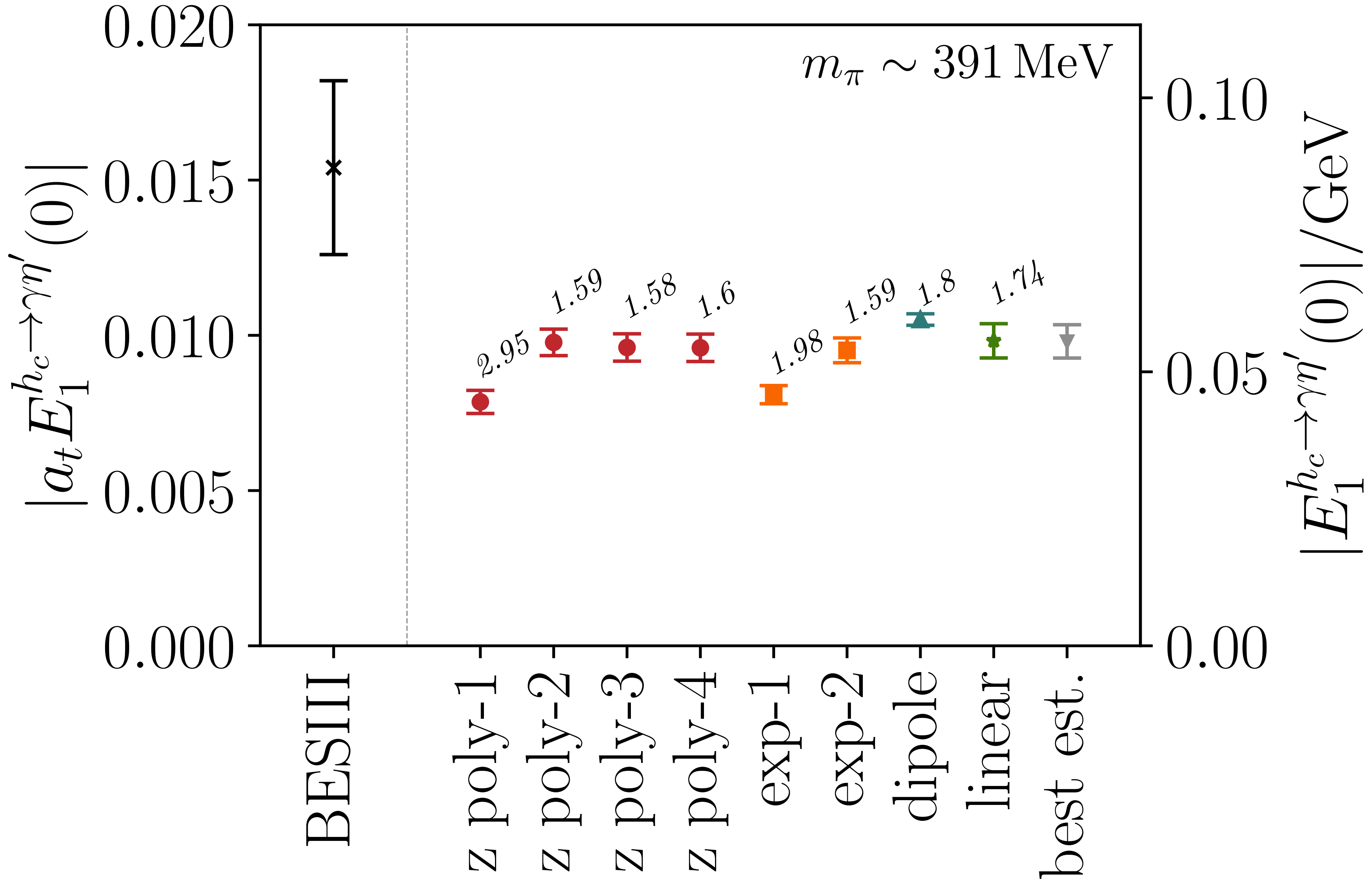

Comparison with BESIII results

Similar discrepancy with experiment for h_c radiative decays

$$\left|\frac{F^{J/\psi\to\gamma\eta'}(0)}{F^{J/\psi\to\gamma\eta}(0)}\right| = 3.3(3) \qquad \left|\frac{E_1^{h_c\to\gamma\eta'}(0)}{E_1^{h_c\to\gamma\eta}(0)}\right| = 2.9(3)$$

singlet-vs-octet hierarchy is reproduced consistently.

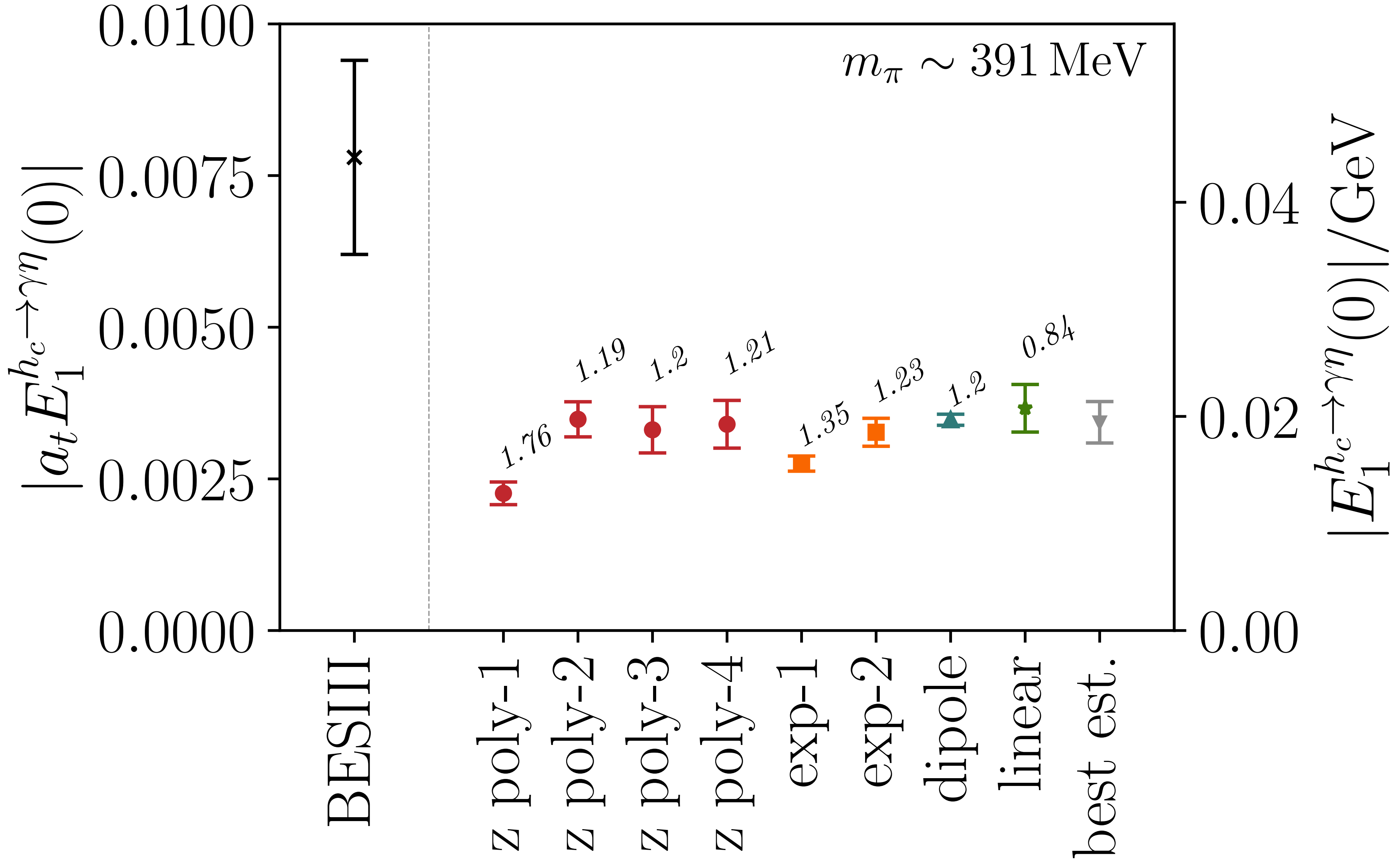

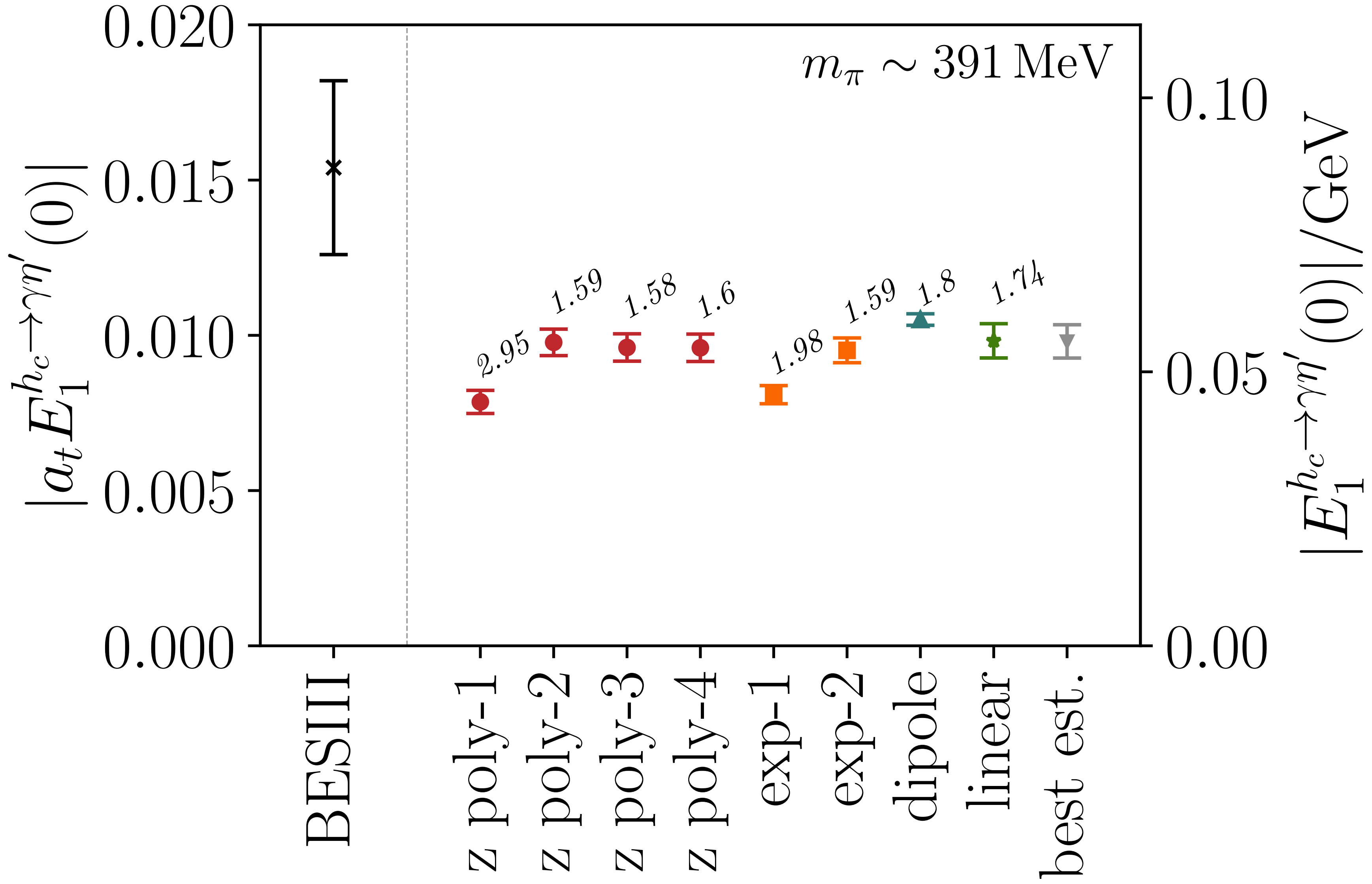

Comparison with BESIII results

Similar discrepancy with experiment for h_c radiative decays

$$\left|\frac{F^{J/\psi\to\gamma\eta'}(0)}{F^{J/\psi\to\gamma\eta}(0)}\right| = 3.3(3) \qquad \left|\frac{E_1^{h_c\to\gamma\eta'}(0)}{E_1^{h_c\to\gamma\eta}(0)}\right| = 2.9(3)$$

singlet-vs-octet hierarchy is reproduced consistently.

A dimensionless ratio that compares the strength of the electric dipole process in h_c decays to the magnetic dipole process in J/ψ decays

$$\left.\frac{|E_1(0)|}{m_{J/\psi}|\mathbf{q}||F(0)|}\right|_{\eta} = 1.84(37)^{\mathrm{expt.}}, 1.76(20)^{391\,\mathrm{MeV}}$$

$$\left.\frac{|E_1(0)|}{m_{J/\psi}|\mathbf{q}||F(0)|}\right|_{\eta'} = 1.58(29)^{\mathrm{expt.}}, 1.63(11)^{391\,\mathrm{MeV}}$$

Discrepancy comes from η/η' properties on this lattice

vacuum topology? light quark mass? $U(1)_A$ anomaly?

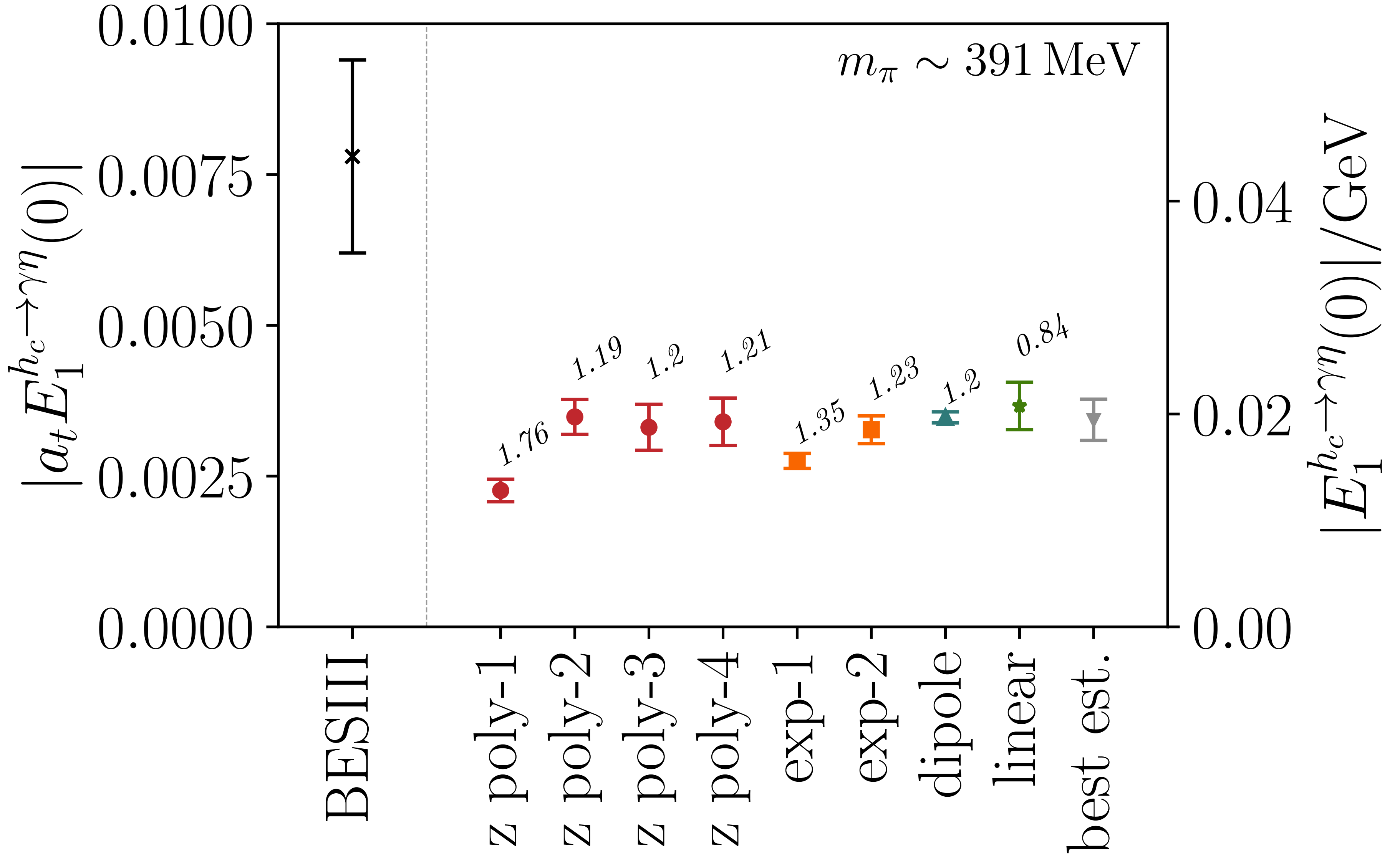

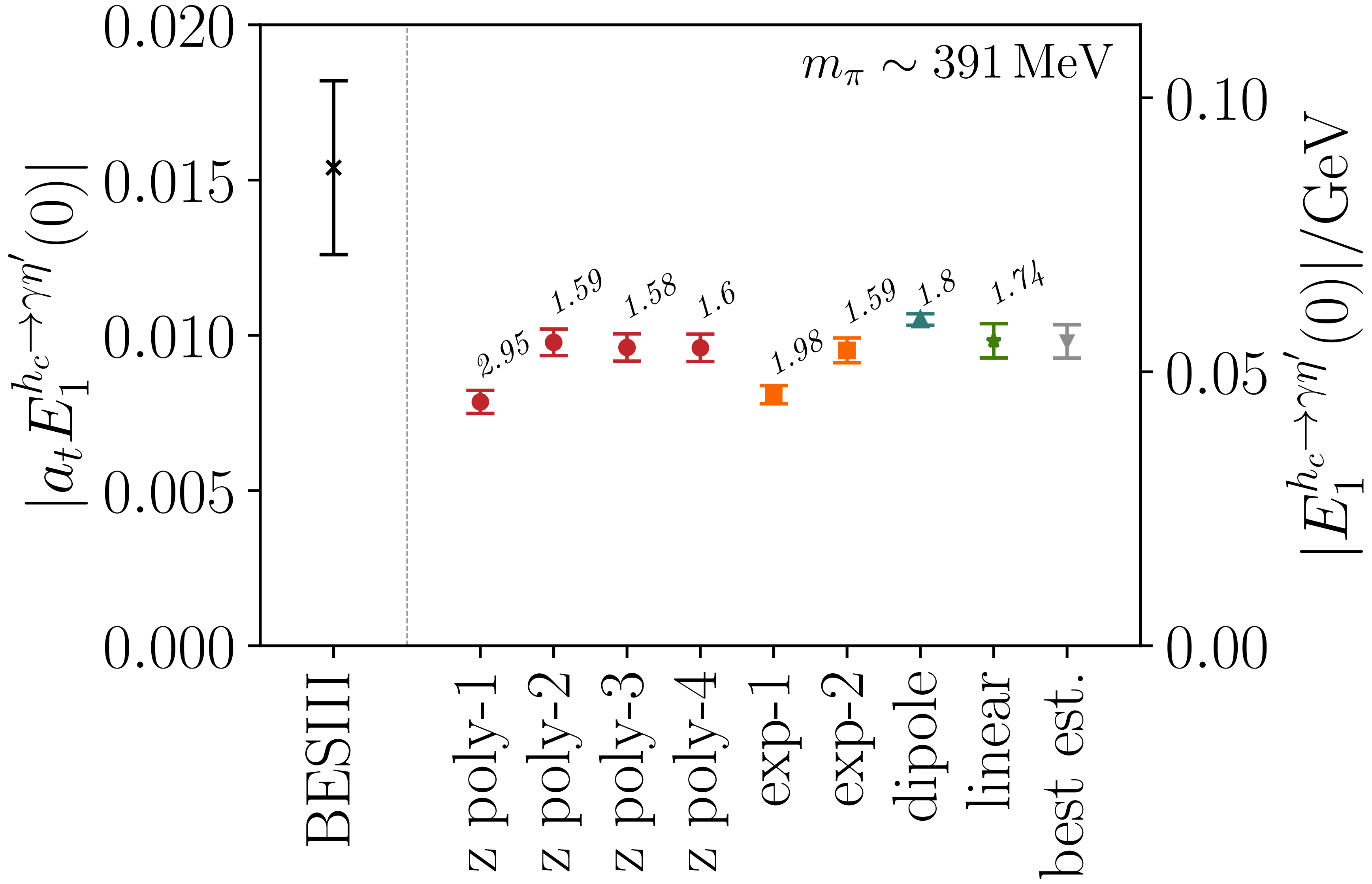

Conclusion

- Using a large operator basis we are able to create operators for both η and η' at high momenta.
- Large range of momenta and irreps allows for many kinematic combinations in the three-point function.
- We are able to extract a clear signal for radiative decays from excited state h_c to excited state η'.
- Good demonstration of the lattice technologies which can be applied to more radiative decays
- Discrepancy with experiment requires calculations on more lattice ensembles to understand fully

Additional Slides

ψ' radiative decays

$\psi' \to \gamma\eta$

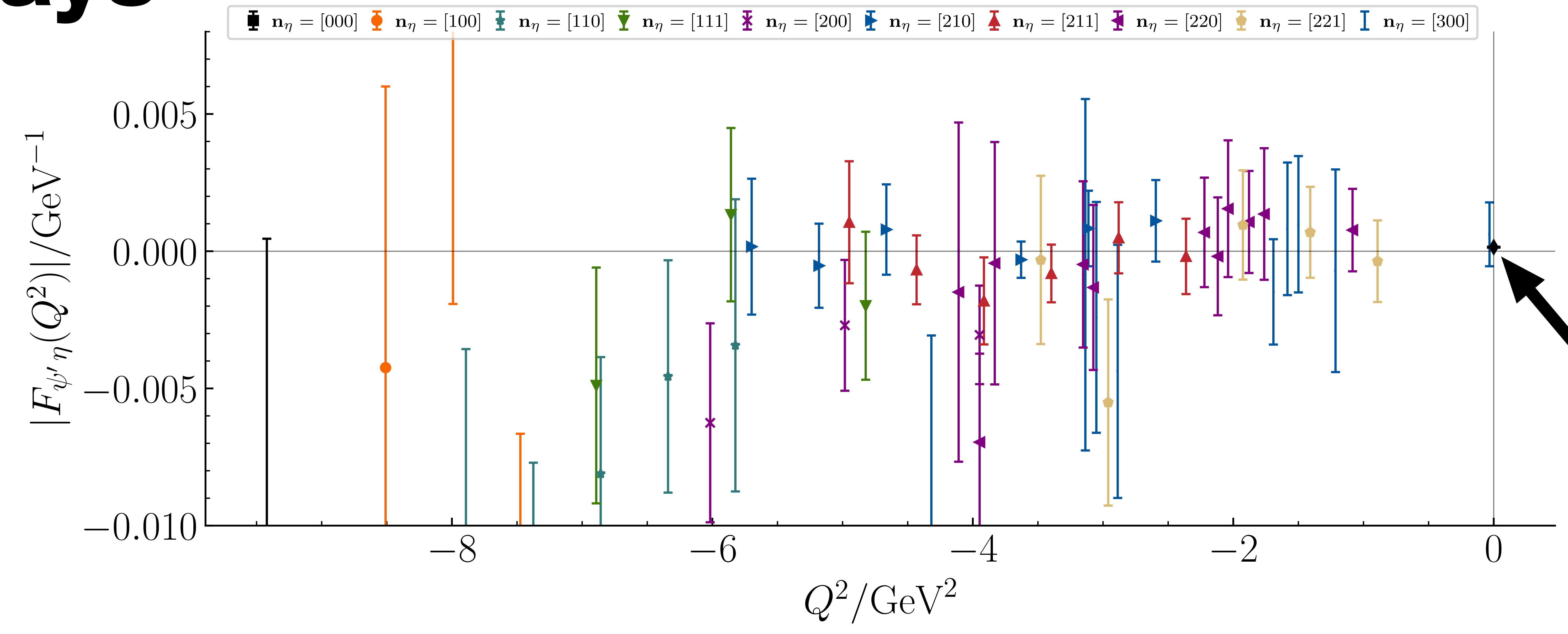

Signal is too small to make out with current statistics

expected value from experiment

$\psi' \to \gamma\eta'$

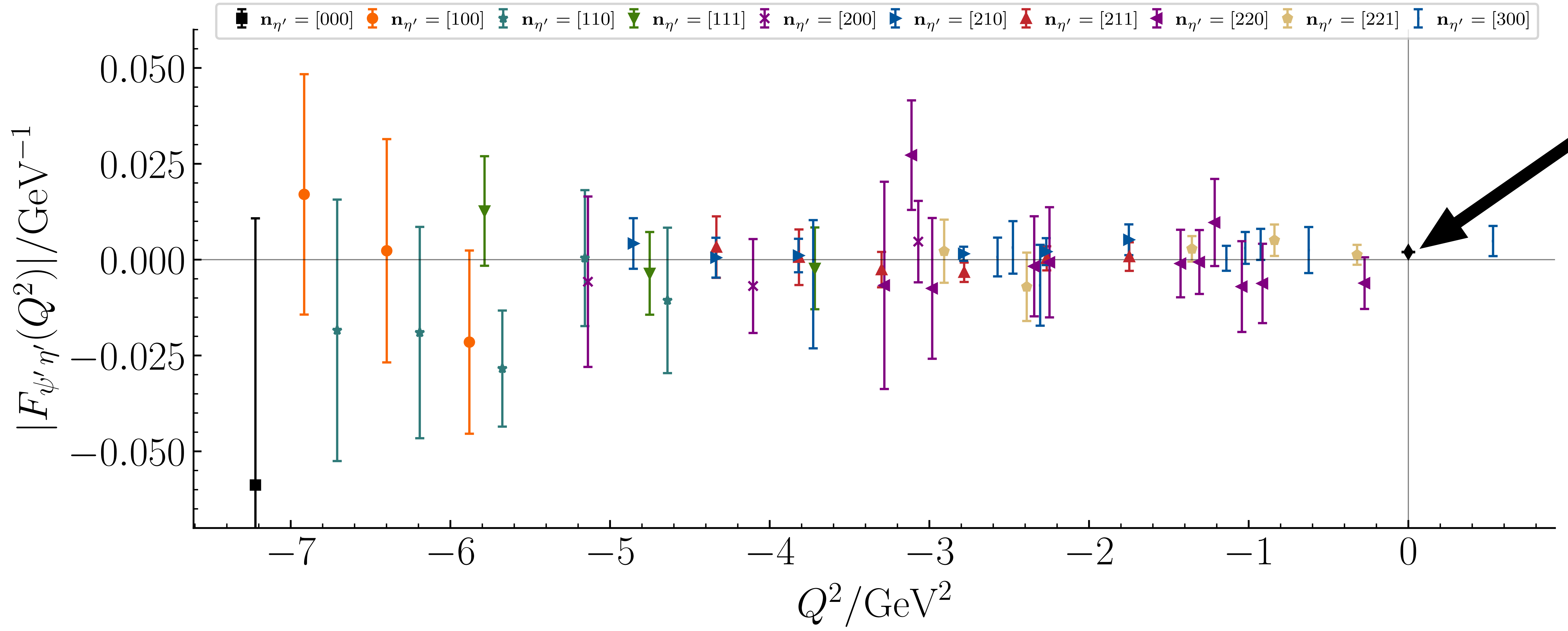

$h_c \to l^+l^-\eta^{(\prime)}$ Dalitz decay

Differential decay rate,

$$\frac{d\Gamma}{dq^2\, d\cos\theta_\ell^\star} = \frac{1}{27}\alpha^2 \frac{|\mathbf{q}|}{m_{h_c}^2} \frac{|\mathbf{p}_\ell^\star|}{\sqrt{q^2}} \frac{1}{q^2} \left[\left(\left(1 + \frac{4m_\ell^2}{q^2}\right)|E_1|^2 + q^2|C_1|^2 \right) + 4\frac{|\mathbf{p}_\ell^\star|^2}{q^2} \left(|E_1|^2 - q^2|C_1|^2 \right) \cos^2\theta_\ell^\star \right]$$

depends on both $|E_1(q^2)|$ and $\sqrt{q^2}\,|C_1(q^2)|$

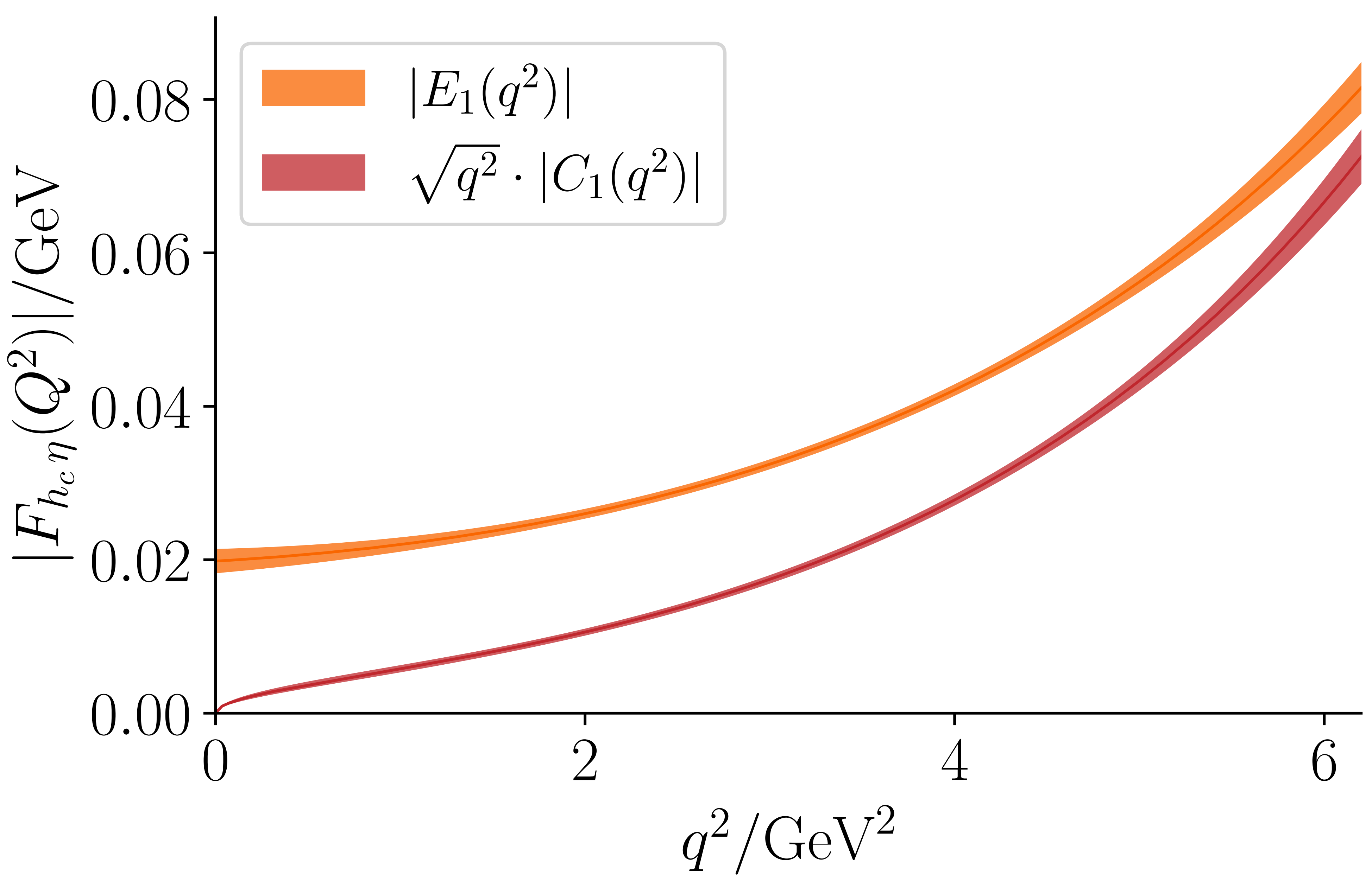

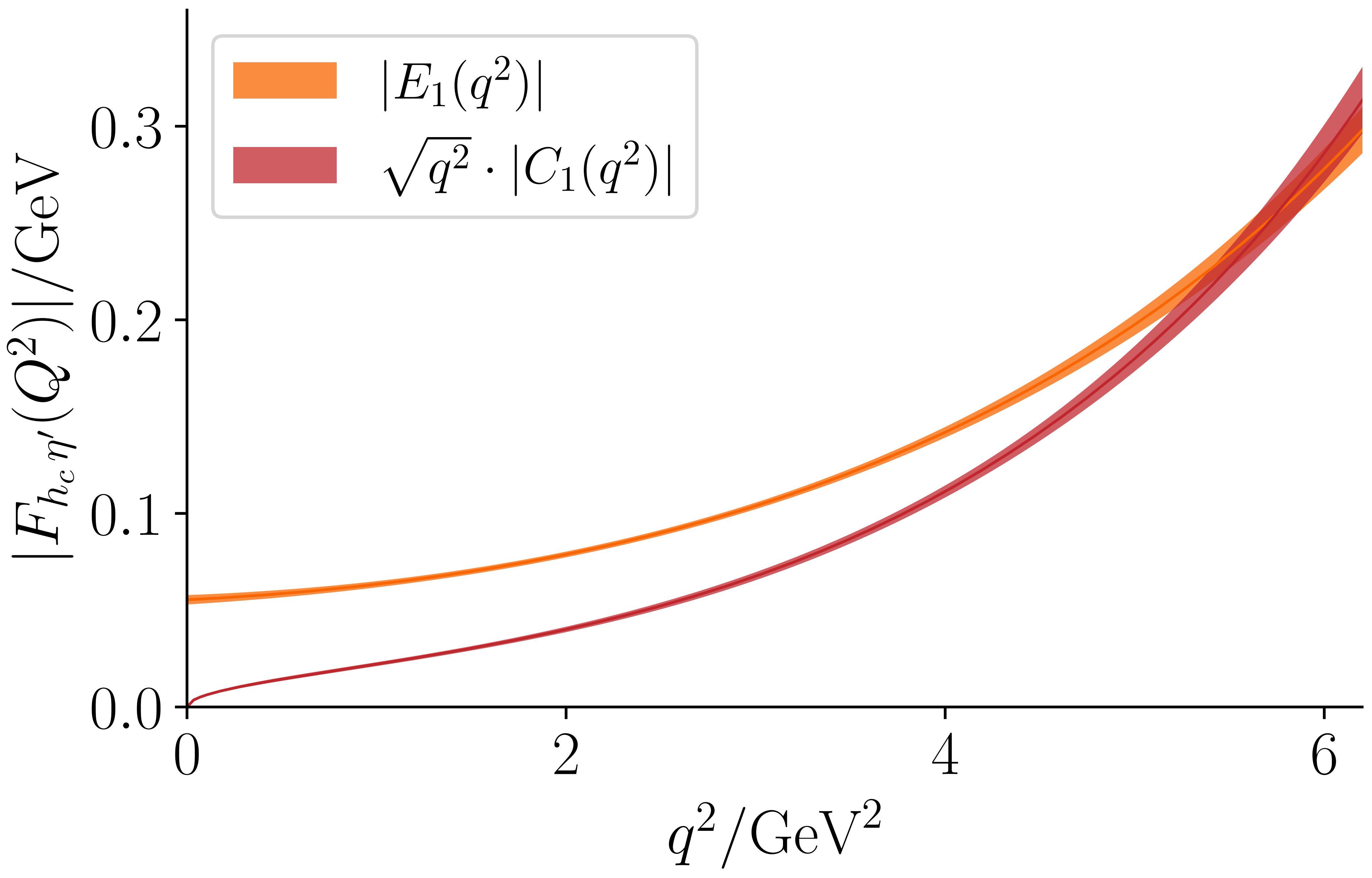

No experimental measurements yet!

Any remaining contributions from excited states?

If we don't average over all matrix elements at each Q^2 point we can compare the cases where the h_c is the ground—state to those where the h_c is an excited—state.

h_c is the ground state in its irrep

h_c is an excited state in its irrep

We see good agreement between the two types of operators over the full range of Q^2 values

$h_c \to \gamma\eta$

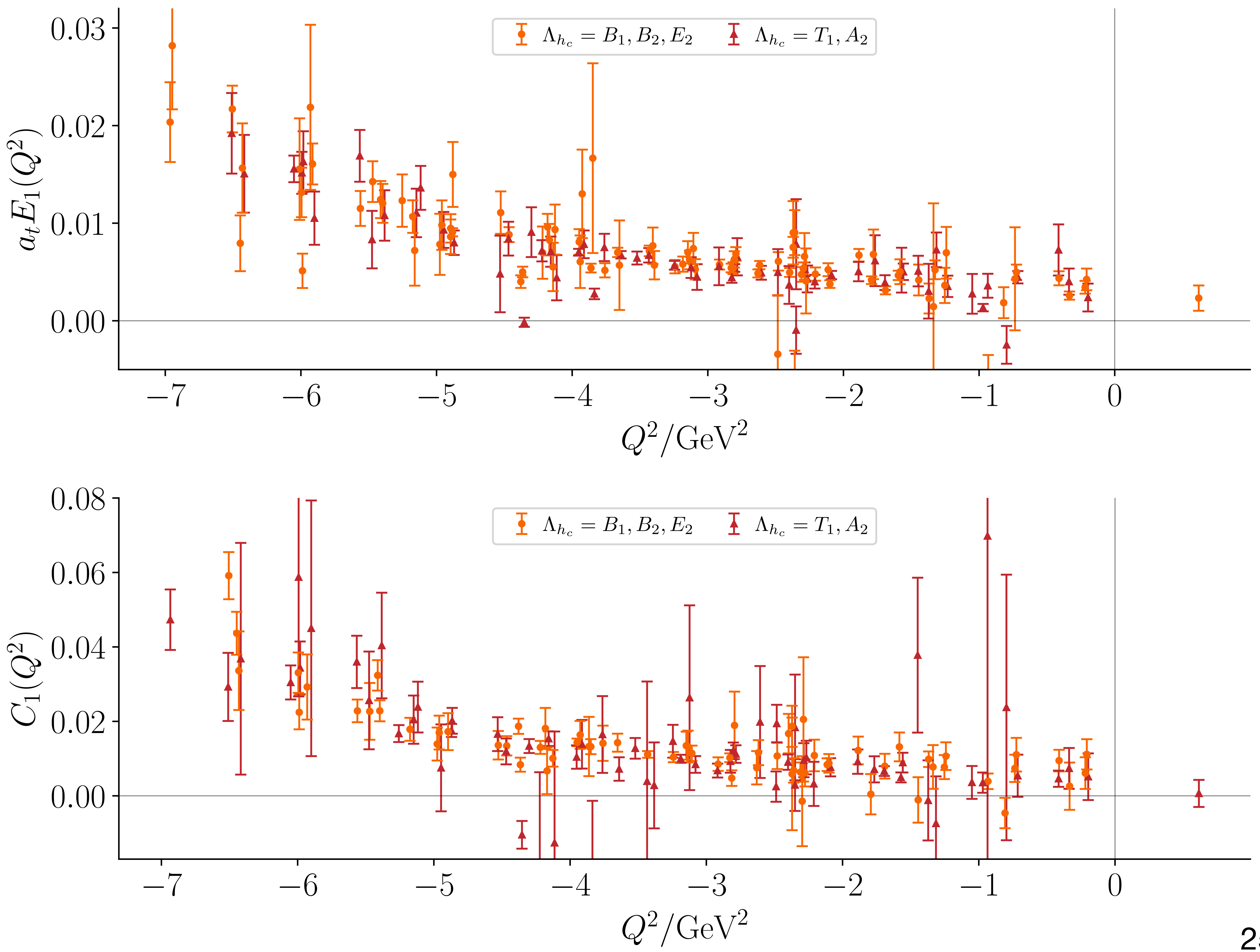

$\mathcal{O}(a)$-improved vector current

~15% correction

$$j_k = Z_V^s\left(\bar{\psi}\gamma_k\psi + \frac{1}{4}(1-\xi)a_t\partial_0(\bar{\psi}\sigma_{0k}\psi)\right)$$

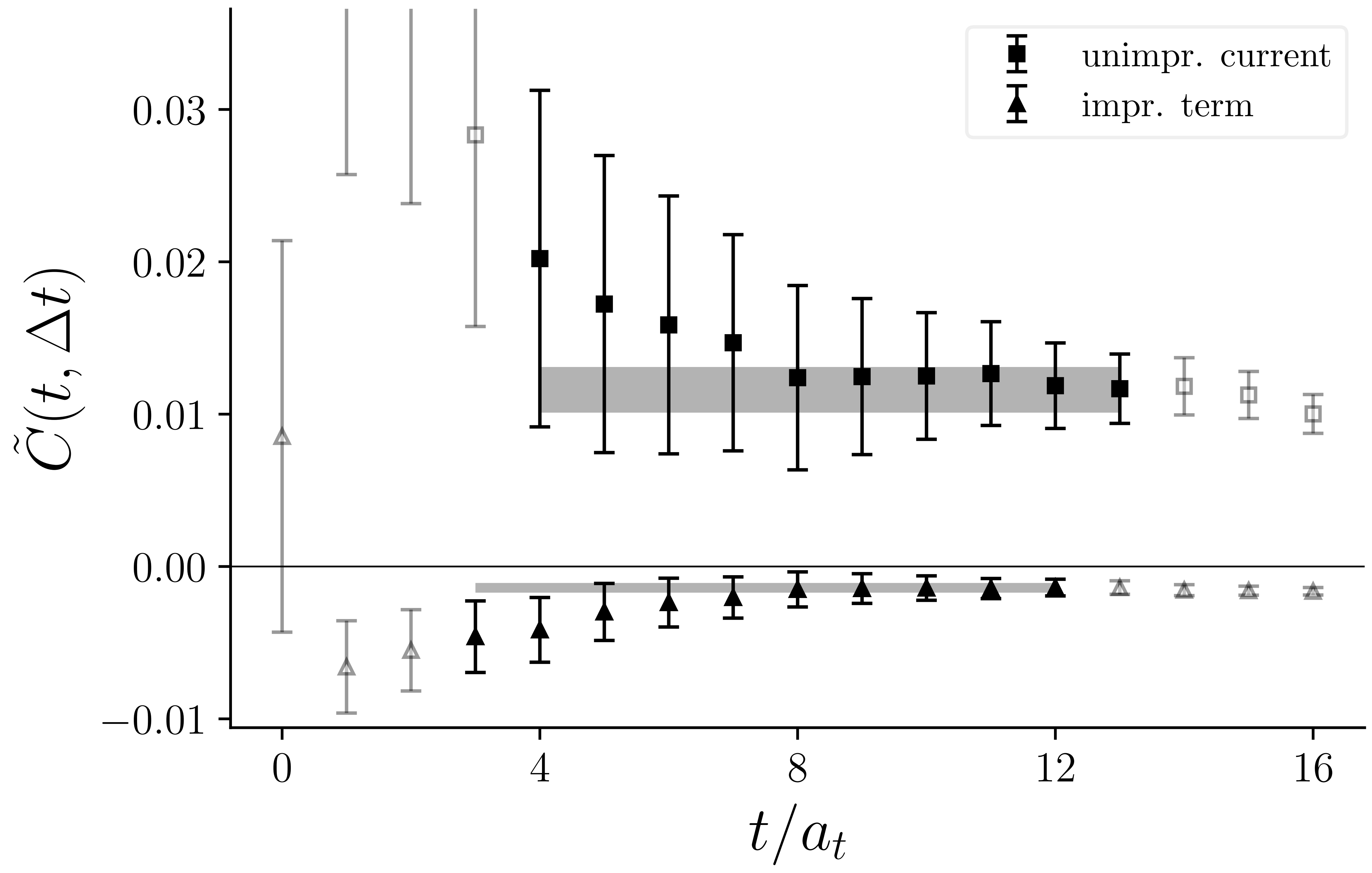

Spatial and temporal currents

- Decent agreement between spatial and temporal currents
- Temporal current has larger errors for most points

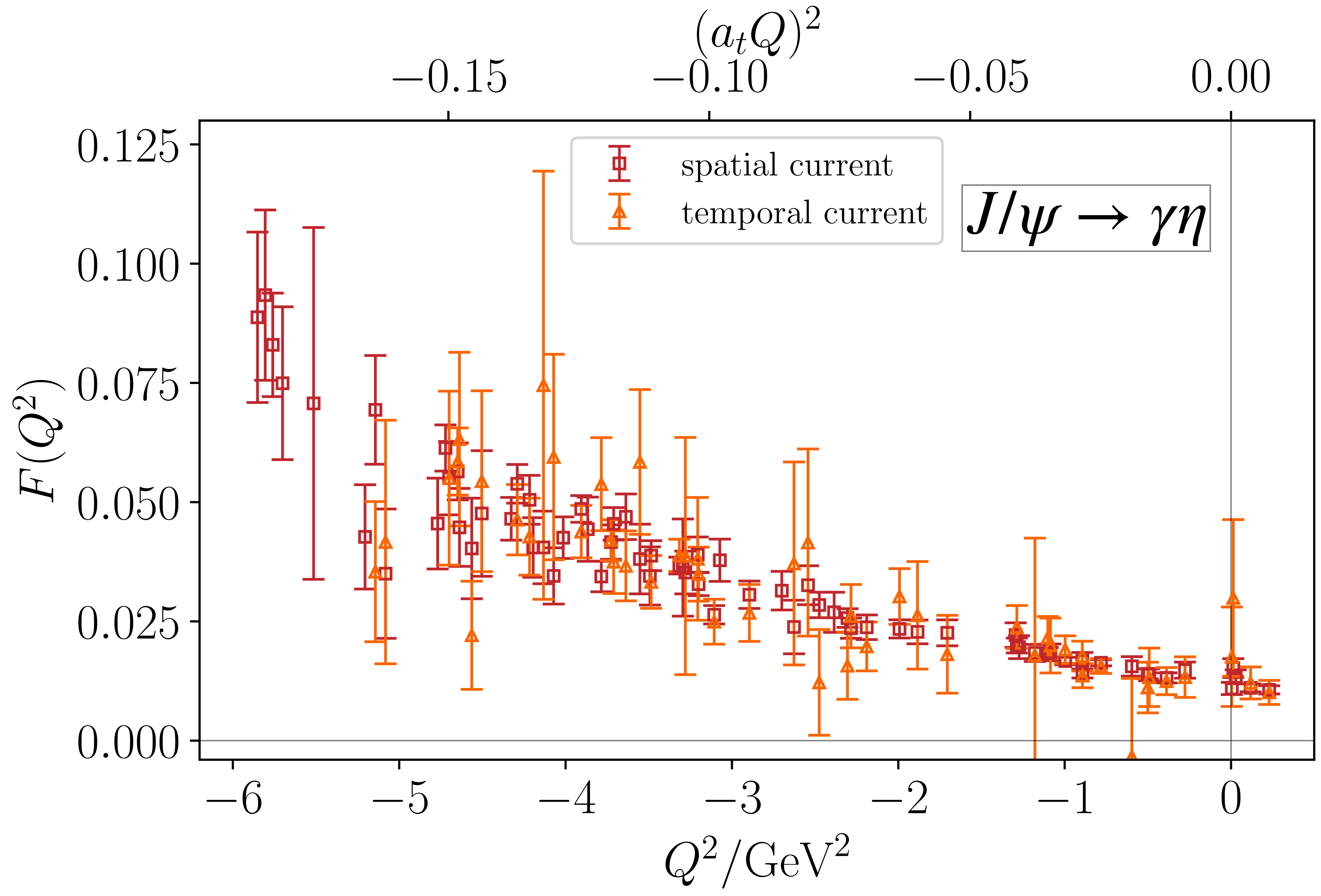

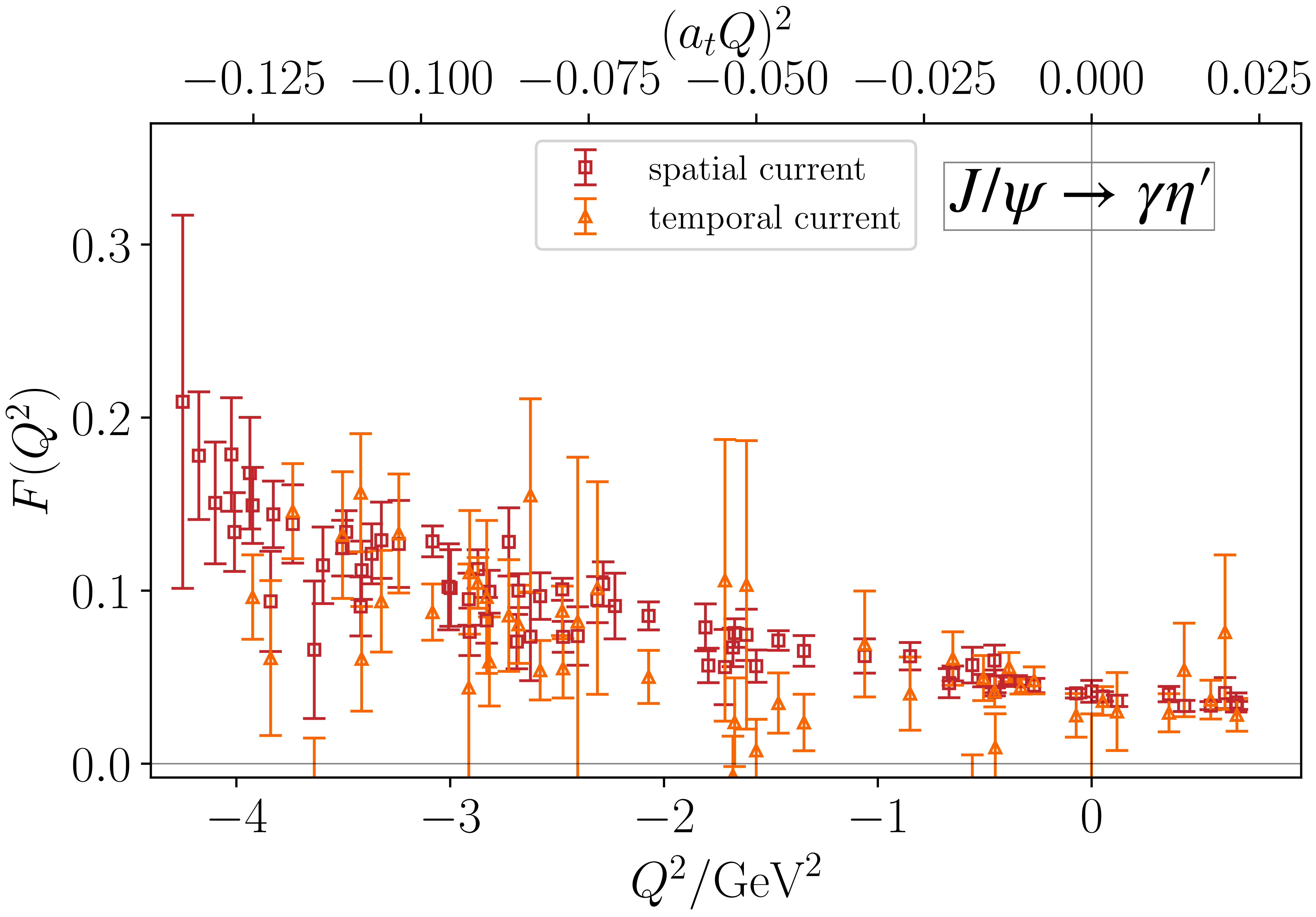

Any remaining contributions from excited states?

- Fitting four different source-sink separations seperately: $\Delta t = (12, 16, 20, 24)a_t$
- Good agreement over the range of Q^2 values

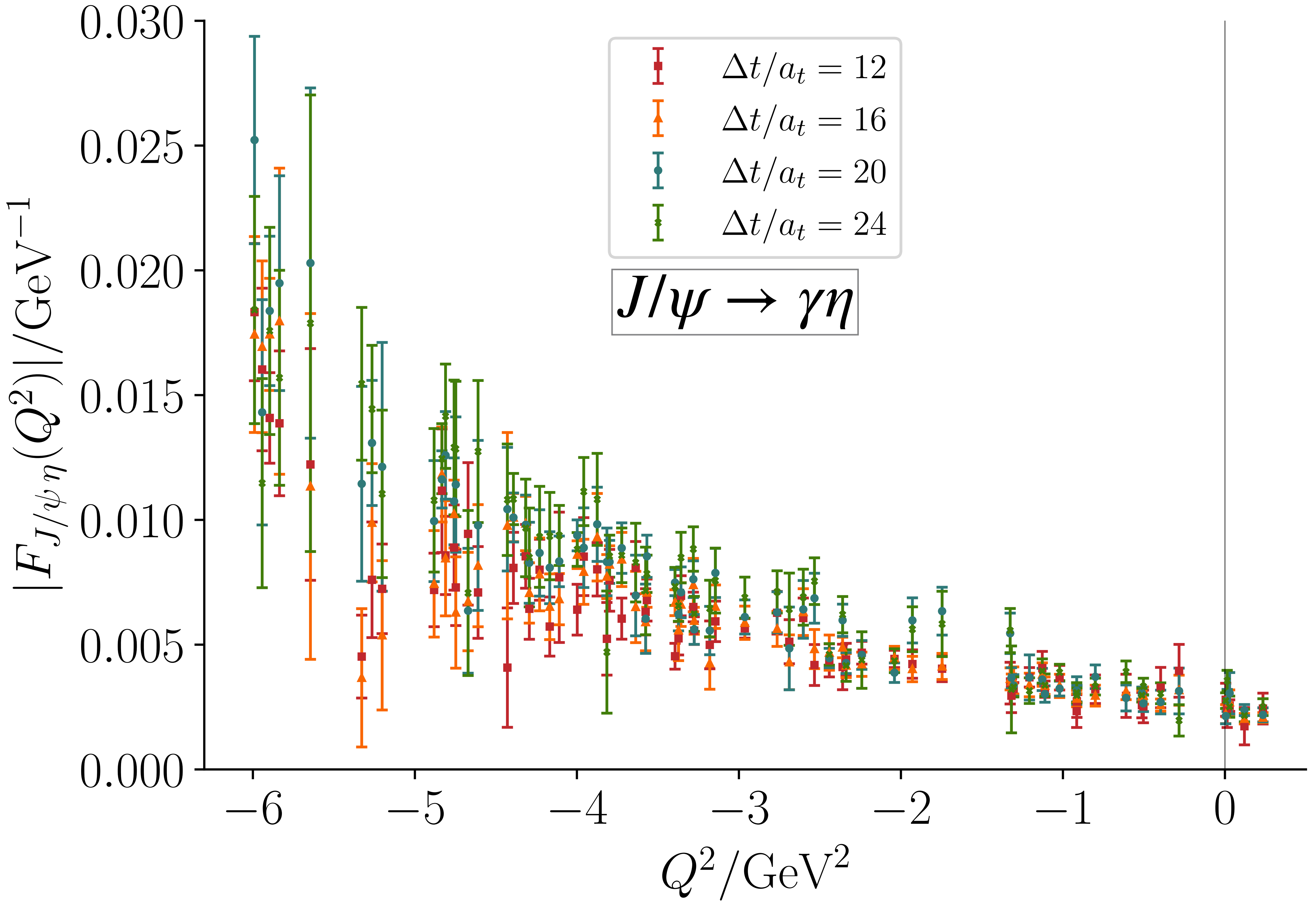

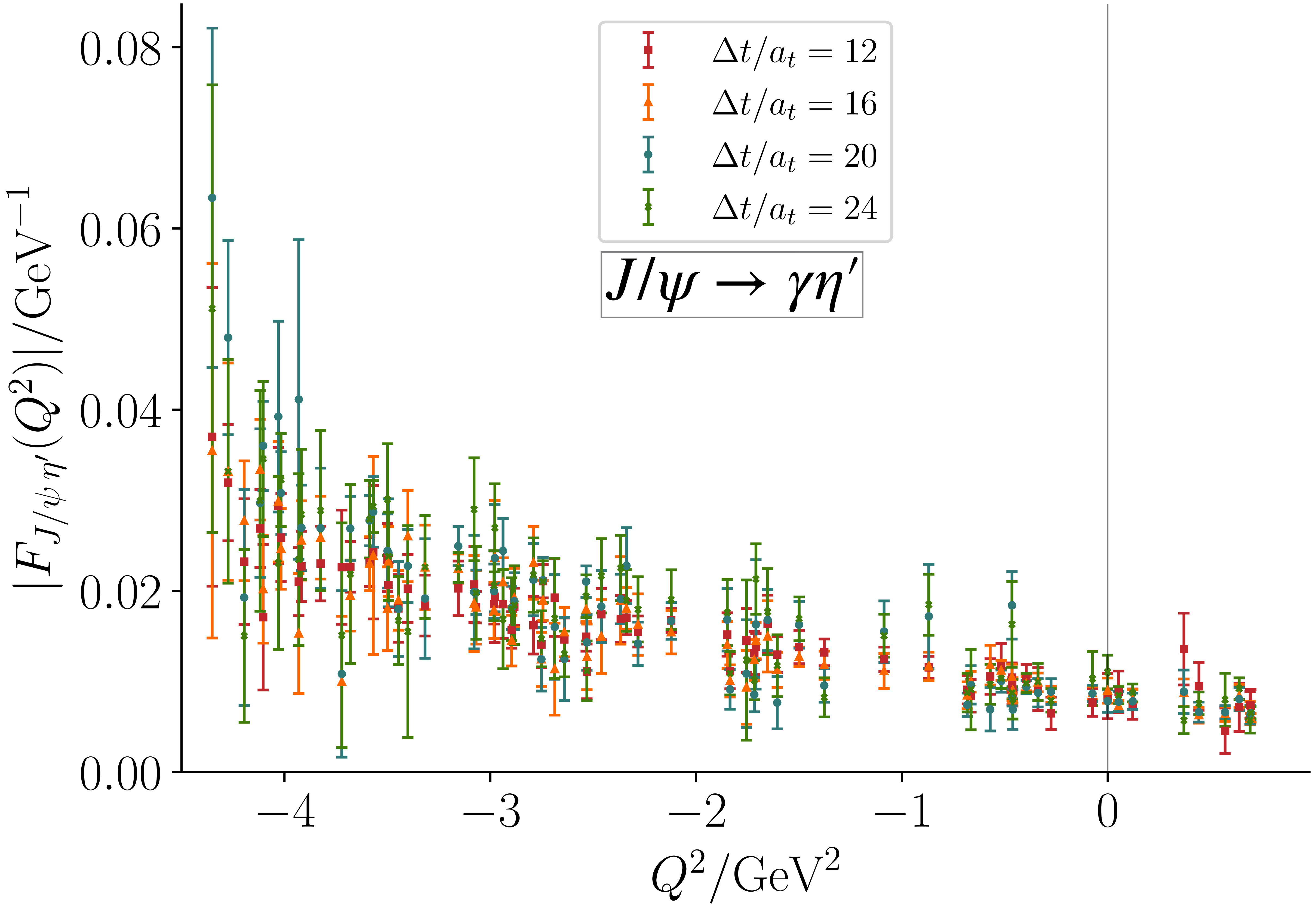

Big improvements on the previous literature

[PRL 130 061901]

Jiang et al. 2023

TABLE I. Parameters of the gauge ensemble.

$L_s^3 \times T$	β	a_t^{-1} (GeV)	ξ	m_π (MeV)	N_{cfg}
$16^3 \times 128$	2.0	6.894(51)	~ 5.3	348.5(1.0)	6991

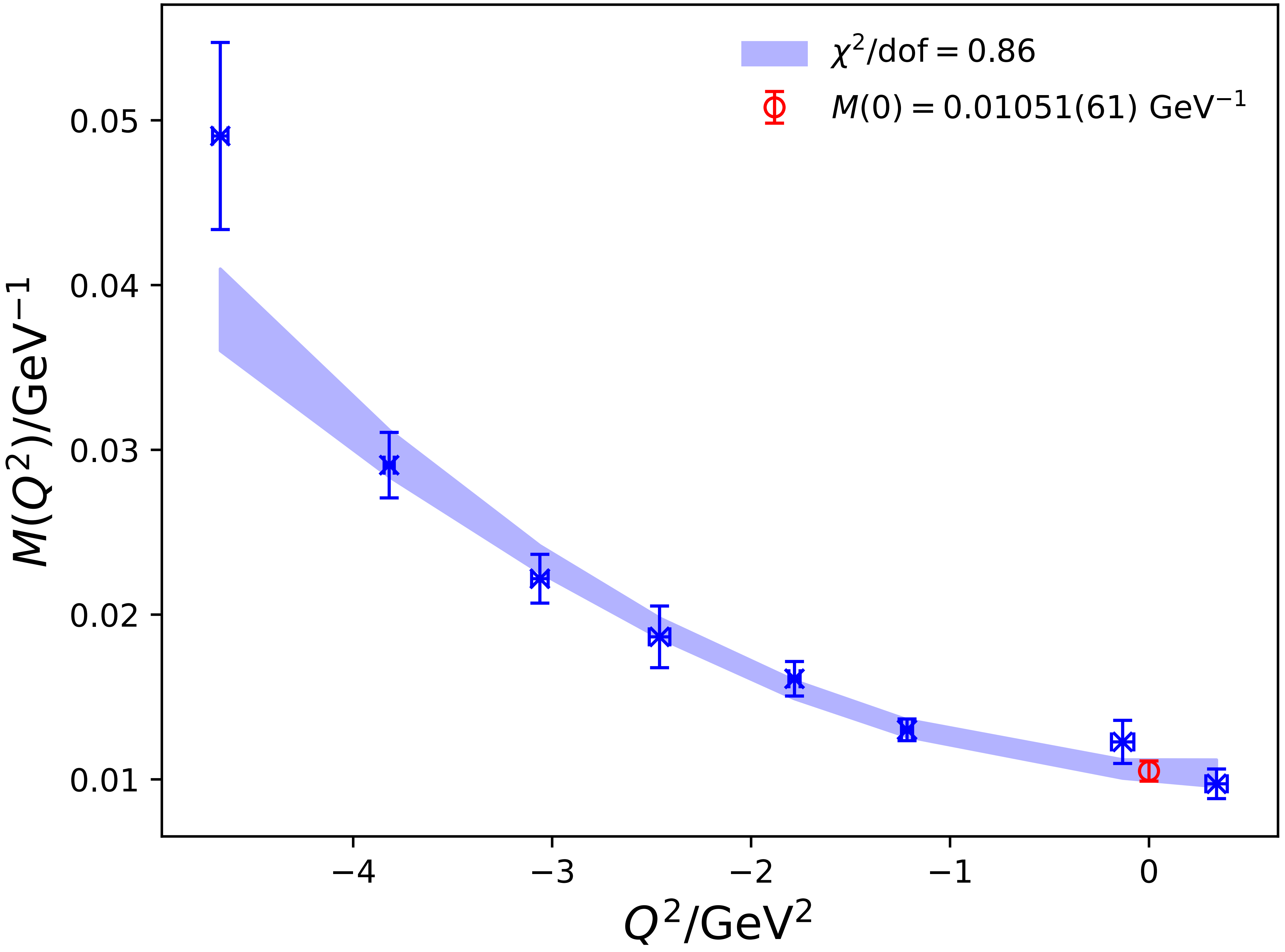

- Only 2 quark flavors
- Limited momentum combinations
- No vector current improvement